

Indirect searches for sterile neutrinos at a high-luminosity Z-factory

A. Abada^a, V. De Romeri^b, S. Monteil^b, J. Orloff^b and A. M. Teixeira^b

^a Laboratoire de Physique Théorique, CNRS – UMR 8627,
Université de Paris-Sud, F-91405 Orsay Cedex, France

^b Laboratoire de Physique Corpusculaire, CNRS/IN2P3 – UMR 6533,
Campus des Cézeaux, 24 Av. des Landais, F-63177 Aubière Cedex, France

Abstract

A future high-luminosity Z -factory will offer the possibility to study rare Z decays, as those leading to lepton flavour violating final states. Processes such as $Z \rightarrow \ell_1^\mp \ell_2^\pm$ are potentially complementary to low-energy (high-intensity) observables of lepton flavour violation. In this work we address the impact of new sterile fermions on lepton flavour violating Z decays, focusing on potential searches at FCC-ee (TLEP), and taking into account experimental and observational constraints on the sterile states. We consider a minimal extension of the Standard Model by one sterile fermion state, and two well-motivated frameworks of neutrino mass generation, the Inverse Seesaw embedded into the Standard Model, and the ν MSM. Our study shows that sterile neutrinos can give rise to contributions to $\text{BR}(Z \rightarrow \ell_1^\mp \ell_2^\pm)$ within reach of the FCC-ee. We also discuss the complementarity between a high-luminosity Z -factory and low-energy charged lepton flavour violation facilities.

1 Introduction

Rare flavour-violating Z decays, as is the case of those violating lepton flavour conservation $Z \rightarrow e\mu, \mu\tau, e\tau$, provide a clear evidence for new physics beyond the Standard Model (SM). In the SM, these decays are forbidden due to the GIM mechanism [1], and their rates remain extremely small (below 10^{-50}) when the SM is minimally (ad-hoc) extended to incorporate flavour violation in the neutral lepton sector (neutrino masses and mixings) [2–5].

Sizeable rates for $Z \rightarrow \ell_1^\mp \ell_2^\pm$ processes reflect the existence of new particles, either coupling with sub-weak strength to the SM particles, or then sufficiently heavy to have escaped direct detection at current high-energy searches. Among these feebly interacting particles, potentially at the origin of $Z \rightarrow \ell_1^\mp \ell_2^\pm$ decays, are sterile (gauge-neutral) fermions, arising in several minimal extensions of the SM, as for instance in those aiming at addressing the origin of neutrino masses and mixings. The existence of sterile states is further supported by current data from neutrino experiments (Gallium [6], reactor [7] and accelerator [8, 9] anomalies). Sterile neutrinos are also

a popular solution for the dark matter (DM) problem [10–12], and can potentially alleviate some tensions regarding structure formation observations [13]. (Although there is still a tension between the most recent Planck results on extra light neutrinos (relics) and reactor anomalies, in this work we focus on the rôle of (heavier) sterile fermions, which are not expected to contribute as light relativistic degrees of freedom [14].) Rare *charged* lepton flavour violating (cLFV) Z decays have been extensively discussed in the context of SM extensions involving massive (Majorana and/or Dirac) neutrinos [5, 15–17]; similar studies were carried using an effective theory approach [18–21], some also exploring a possible complementarity with low-energy cLFV searches.

The current bounds on the branching ratios (BRs) for cLFV Z decays,

$$\text{BR}(Z \rightarrow \ell_1^\mp \ell_2^\pm) = \frac{\Gamma(Z \rightarrow \ell_1^\pm \ell_2^\mp)}{\Gamma_Z}, \quad (1)$$

were established by LEP, performing as a Z factory; recently, the ATLAS experiment established new bounds on the corresponding BRs, significantly improving the bound for $e\mu$ final states:

$$\text{BR}(Z \rightarrow e^\mp \mu^\pm) < 7.5 \times 10^{-7} \quad [22], \quad (2)$$

$$\text{BR}(Z \rightarrow e^\mp \tau^\pm) < 9.8 \times 10^{-6} \quad [23, 24], \quad \text{BR}(Z \rightarrow \mu^\mp \tau^\pm) < 1.2 \times 10^{-5} \quad [24, 25]. \quad (3)$$

A future circular collider, running in electron-positron mode, FCC-ee (TLEP) [26], will constitute a true high-luminosity Z factory, with an expected production of 10^{12} Z bosons (10^{13} with the “crab-waist”), when operating at the Z mass pole. Such large statistics (above Tera- Z) will thus allow to better determine the properties of the Z boson, and to probe new physics (NP) scenarios through the above cLFV processes. The clean nature of the cLFV $Z \rightarrow \ell_1^\mp \ell_2^\pm$ decays (only charged leptons - especially muons - in the final state) implies that the sensitivity to these rare processes is essentially only constrained by the expected luminosity; one can thus foresee a significant improvement in the experimental sensitivity at FCC-ee to rare cLFV Z decays, for instance, $\text{BR}(Z \rightarrow e^\mp \mu^\pm) \sim 10^{-13}$.

Revisiting cLFV Z decays in the presence of extra sterile fermions is particularly timely given the present experimental context: not only we have reached an unprecedented precision in the determination of several neutrino oscillation parameters [27–32], and new bounds on low-energy cLFV observables (for instance MEG [33]), but we are also entering a challenging era, where many ambitious (post-LHC) experimental projects are being put forward. Given their rôle in a vast array of observables (see, for instance [34–36] and references therein), sterile neutrinos are becoming strong candidates for the physics case of several post-LHC facilities, as is the case of the FCC-ee (TLEP). It is also worth mentioning that direct searches for (nearly) sterile fermions, as right-handed (RH) neutrinos, relying on their comparatively long lifetime, have recently been studied in the context of high-luminosity Z -factories like the FCC-ee [37].

The present work focuses on the potential of the FCC-ee to explore the rôle of cLFV decays of the Z boson as indirect probes of sterile fermions [26], emphasising the complementarity of these searches with respect to low-energy cLFV observables such as $\mu \rightarrow e\gamma$ and $\mu \rightarrow eee$ decays and $\mu - e$ conversion in nuclei. We consider SM extensions via sterile neutrinos, with a non-negligible mixing to the light (mostly) active neutrinos, for a wide range of masses of the sterile mass spectrum. In particular, we address three scenarios: a simple toy-model extension of the SM with one sterile fermion (the “3+1 model”), and two well motivated frameworks for neutrino mass generation, the ν MSM [38] and one realisation of the Inverse Seesaw [39].

Our analysis (conducted for each of the above mentioned scenarios, which are confronted to all observational and experimental constraints, especially those from low-energy cLFV observables),

reveals that sterile neutrinos can indeed give rise to contributions to $\text{BR}(Z \rightarrow \ell_1^\mp \ell_2^\pm)$ within reach of the FCC-ee.

This work is organised as follows: in Section 2 we consider the general formulation of the lepton flavour violating (and lepton flavour conserving) $\text{BR}(Z \rightarrow \ell^\mp \ell^\pm)$ in terms of the sterile masses and mixings to the active neutrinos. We also discuss the experimental prospects. In Section 3 we motivate this class of extensions and discuss the different observational (mainly the cosmological ones) and experimental bounds on sterile states. In the following three sections, we describe and discuss in detail the prospects of different extensions of the SM regarding $Z \rightarrow \ell_1^\mp \ell_2^\pm$ decays at a high-luminosity Z factory, also addressing the complementarity with respect to other low-energy observables.

2 Leptonic Z decays in the presence of sterile neutrinos

In the original formulation of the SM with massless neutrinos and no mixing in the lepton sector, the couplings of the gauge bosons to neutral and charged leptons are strictly flavour conserving, lepton-flavour changing Z decays being forbidden due to the GIM mechanism [1]. Moreover, the couplings are flavour universal, so that in the SM one has $g_{\ell_i \nu_i W} \propto g_w$, $g_{\ell_i \ell_i Z} \propto g_w$, as well as $g_{\nu_i \nu_i Z} \propto g_w$, where g_w denotes the weak coupling constant. These rates remain extremely small even in the case in which the SM is “ad-hoc”-extended to incorporate three massive and mixing neutrinos [2–5, 17]:

$$\text{BR}(Z \rightarrow \mu^\mp \tau^\pm) \sim 10^{-54}, \quad \text{BR}(Z \rightarrow e^\mp \mu^\pm) \sim \text{BR}(Z \rightarrow e^\mp \tau^\pm) \lesssim 4 \times 10^{-60}. \quad (4)$$

Let us now consider the extension of the SM via n_S additional sterile neutral (Majorana) fermions, mixing with the active neutrinos. In the physical lepton (or mass) basis, the SM Lagrangian is modified as follows¹:

$$\begin{aligned} \mathcal{L}_{W^\pm} &= -\frac{g_w}{\sqrt{2}} W_\mu^- \sum_{l=1}^3 \sum_{j=1}^{3+n_S} \mathbf{U}_{lj} \bar{\ell}_l \gamma^\mu P_L \nu_j + \text{h.c.}, \\ \mathcal{L}_{Z^0} &= -\frac{g_w}{2 \cos \theta_w} Z_\mu \sum_{i,j=1}^{3+n_S} \bar{\nu}_i \gamma^\mu (P_L \mathbf{C}_{ij} - P_R \mathbf{C}_{ij}^*) \nu_j, \\ \mathcal{L}_{H^0} &= -\frac{g_w}{2M_W} H \sum_{i,j=1}^{3+n_S} \mathbf{C}_{ij} \bar{\nu}_i (P_R m_i + P_L m_j) \nu_j + \text{h.c.}, \\ \mathcal{L}_{G^0} &= \frac{ig_w}{2M_W} G^0 \sum_{i,j=1}^{3+n_S} \mathbf{C}_{ij} \bar{\nu}_i (P_R m_j - P_L m_i) \nu_j + \text{h.c.}, \\ \mathcal{L}_{G^\pm} &= -\frac{g_w}{\sqrt{2}M_W} G^- \sum_{l=1}^3 \sum_{j=1}^{3+n_S} \mathbf{U}_{lj} \bar{\ell}_l (m_i P_L - m_j P_R) \nu_j + \text{h.c.} \end{aligned} \quad (5)$$

where $P_{L,R} = (1 \mp \gamma_5)/2$. As is clear from the above equations, flavour is violated by mixings in both charged and neutral current interactions. Denoting by $l = 1, \dots, 3$ the flavour of the charged leptons, and by $i, j = 1, \dots, 3 + n_S$ the physical neutrino states, the mixing in charged current interactions is parametrized by a rectangular $3 \times (3 + n_S)$ mixing matrix, \mathbf{U}_{lj} . Notice that in the

¹See e.g. [17] for a detailed derivation starting from explicit lepton mass matrices.

case of three neutrino generations, and assuming alignment of the charged lepton's weak and mass basis, \mathbf{U} corresponds to the (unitary) PMNS matrix, U_{PMNS} . For $n_\nu > 3$ ($n_S \geq 1$), the mixing between the left-handed leptons, which we will subsequently denote by \tilde{U}_{PMNS} , corresponds to a 3×3 block of \mathbf{U} . One can parametrize the \tilde{U}_{PMNS} mixing matrix as [40]

$$U_{\text{PMNS}} \rightarrow \tilde{U}_{\text{PMNS}} = (\mathbb{1} - \eta) U_{\text{PMNS}}, \quad (6)$$

where the matrix η encodes the deviation of \tilde{U}_{PMNS} from unitarity [41, 42], due to the presence of extra fermion states. It is also convenient to introduce the invariant quantity $\tilde{\eta}$, defined as

$$\tilde{\eta} = 1 - |\text{Det}(\tilde{U}_{\text{PMNS}})|, \quad (7)$$

particularly useful to illustrate the effect of the new active-sterile mixings (corresponding to a deviation from unitarity of the \tilde{U}_{PMNS}).

As can be seen from above, the mixing in the neutral lepton sector induced by the Majorana states also opens the possibility for flavour violation in neutral currents; this is encoded in a square $(3 + n_S) \times (3 + n_S)$ mixing matrix

$$\mathbf{C}_{ij} = \sum_{l=1}^3 \mathbf{U}_{li}^* \mathbf{U}_{lj}. \quad (8)$$

2.1 Rare lepton flavor violating Z decays revisited

One of the main features of the SM extended by sterile Majorana neutrinos, which mix with the active ones, is thus the possibility of flavour violating $Z\nu_i\nu_j$ interactions (flavour-changing neutral currents), coupling both the left- and right-handed components of the neutral fermions to the Z boson. Together with the charged-current LFV couplings ($\propto \tilde{U}_{\text{PMNS}}$), these interactions will induce an effective *charged* lepton-flavour violating vertex $Z\ell_1^\mp\ell_2^\pm$. We depict the full set of one-loop diagrams in Fig. 1.

Taking into account the contributions of all above higher order processes, the branching ratio for cLFV Z decays (cf. Eq. (1)) is given by [5, 16–20]:

$$\text{BR}(Z \rightarrow \ell_1^\mp \ell_2^\pm) = \frac{\alpha_W^3}{192\pi^2 c_W^2} \frac{M_Z}{\Gamma_Z} |\mathcal{F}(M_Z^2)|^2 \approx 10^{-6} |\mathcal{F}(M_Z^2)|^2, \quad \text{with } \ell_1 \neq \ell_2. \quad (9)$$

The form factor $\mathcal{F}(Q^2)$ encodes the details of the new interaction and therefore the contribution of the sterile neutrinos:

$$\mathcal{F}(Q^2) = \sum_{i,j=1}^{n_\nu} \mathbf{U}_{l_1 i} \mathbf{U}_{l_2 j}^* V_Z(x_i, x_j, x_Q), \quad (10)$$

where $V_Z(x_i, x_j, x_Q)$ is the vertex function, fully describing the amplitude, and which depends quadratically on the neutrino masses. In the previous expression, we have introduced the mass ratios² $x_i = m_{\nu_i}^2/M_W^2$ and the virtuality of the Z boson $x_Q = Q^2/M_W^2$ (i.e., $x_Z = M_Z^2/M_W^2$ when it is on-shell). In the 't Hooft-Feynman gauge, all diagrams of Fig. 1 [5, 16–20] contribute to the amplitude V_Z :

$$V_Z(x_i, x_j, x_Q) = v_{W\nu\nu}(i, j) + v_{WW\nu}(i) + v_{\phi\nu\nu}(i, j) + v_{\phi\phi\nu}(i) + v_{W\phi\nu}(i) + v_{\text{SelfE}}(i), \quad (11)$$

²The negligible effect of the final state charged lepton masses is ignored for simplicity here.

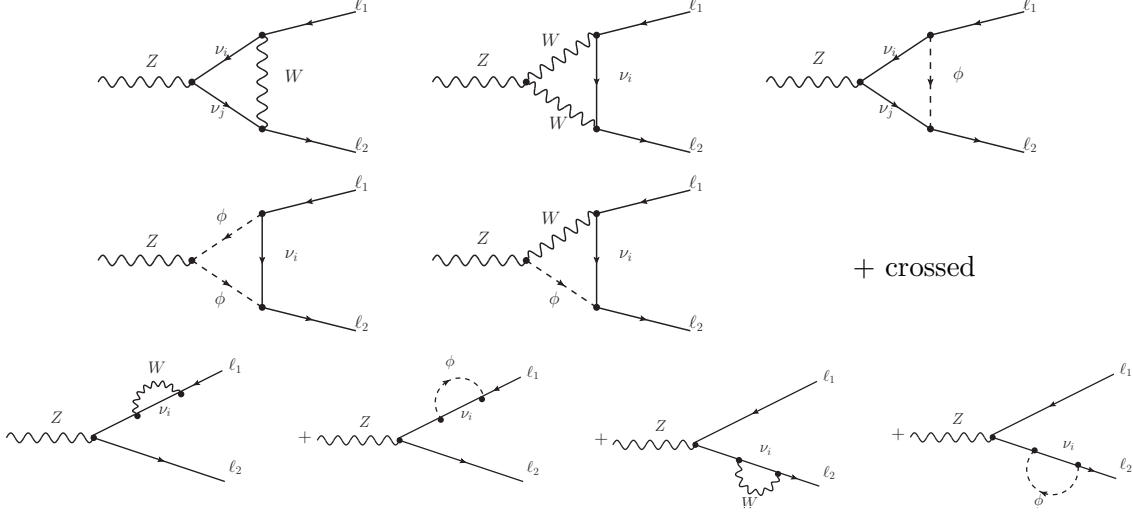


Figure 1: Feynman diagrams for the charged lepton-flavour changing Z decay. From left to right, top to bottom: $v_{W\nu\nu}(i, j)$, $v_{WW\nu}(i)$, $v_{\phi\nu\nu}(i, j)$, $v_{\phi\phi\nu}(i)$, $v_{W\phi\nu}(i)$. The last row contains the self-energy corrections to the external fermion legs, $v_{\text{Self}}(i)$.

with the different contributions given in terms of dimensionless one-loop tensor integrals³ \mathbb{C}_0 , $\bar{\mathbb{C}}_0$, \mathbb{C}_{ab} , $\bar{\mathbb{C}}_{ab}$ and \mathbb{B}_1 [45, 46], listed in Appendix A,

$$v_{W\nu\nu}(i, j) = -\mathbf{C}_{ij} [x_Q (\mathbb{C}_0 + \mathbb{C}_{11} + \mathbb{C}_{12} + \mathbb{C}_{23}) - 2\mathbb{C}_{24} + 1] + \mathbf{C}_{ij}^* \sqrt{x_i x_j} \mathbb{C}_0, \quad (12)$$

$$v_{WW\nu}(i) = 2c_W^2 (2I_3^{iL}) [x_Q (\bar{\mathbb{C}}_{11} + \bar{\mathbb{C}}_{12} + \bar{\mathbb{C}}_{23}) - 6\bar{\mathbb{C}}_{24} + 1], \quad (13)$$

$$v_{\phi\nu\nu}(i, j) = -\mathbf{C}_{ij} \frac{x_i x_j}{2} \mathbb{C}_0 + \mathbf{C}_{ij}^* \frac{\sqrt{x_i x_j}}{2} \left[x_Q \mathbb{C}_{23} - 2\mathbb{C}_{24} + \frac{1}{2} \right], \quad (14)$$

$$v_{\phi\phi\nu}(i) = -(1 - 2s_W^2) (2I_3^{iL}) x_i \bar{\mathbb{C}}_{24}, \quad (15)$$

$$v_{W\phi\nu}(i) = -2s_W^2 (2I_3^{iL}) x_i \bar{\mathbb{C}}_0, \quad (16)$$

$$v_{\text{Self}}(i) = \frac{1}{2} (v_i + a_i - 4c_W^2 a_i) [(2 + x_i) \mathbb{B}_1 + 1]. \quad (17)$$

In the above, the weak neutral vector and axial-vector couplings are defined as

$$v_i = I_3^{iL} - 2Q_i s_W^2, \quad (18)$$

$$a_i = I_3^{iL}, \quad (19)$$

with s_W (c_W) denoting $\sin \theta_W$ ($\cos \theta_W$), Q_i the electric charge and I_3^{iL} the third component of weak isospin.

2.2 Lepton flavour universality in Z decays

As mentioned before, in the SM the charged lepton couplings to the Z boson are strictly flavour universal. Due to the τ lepton mass, $\Gamma(Z \rightarrow \tau^+ \tau^-)$ slightly differs from $\Gamma(Z \rightarrow \ell^+ \ell^-)$, with

³The tensor integrals are numerically evaluated via `LoopTools` [43], based on the `FF` [44] package, which are linked to a private fortran code.

$\ell = e, \mu$ (see, e.g. [47])

$$\Gamma(Z \rightarrow \ell^+ \ell^-) = 0.08397, \quad \Gamma(Z \rightarrow \tau^+ \tau^-) = 0.08378. \quad (20)$$

The current experimental bound from LEP regarding (non-)universality of Z decays into electrons and muons is [48]

$$\frac{\Gamma_Z^{\mu\mu, \text{SM}}}{\Gamma_Z^{ee, \text{SM}}} = 1.0009 \pm 2.8 \times 10^{-3}. \quad (21)$$

Assuming that the electron- and muon- partial widths are equal ($\Gamma_Z^{ee, \text{SM}} = \Gamma_Z^{\mu\mu, \text{SM}}$) we can define the following observable

$$\Delta R_Z^{\text{lep}} = 1 - \frac{\left(1 + \frac{\Gamma_Z^{\mu\mu, \text{NP}}}{\Gamma_Z^{\mu\mu, \text{SM}}}\right)}{\left(1 + \frac{\Gamma_Z^{ee, \text{NP}}}{\Gamma_Z^{ee, \text{SM}}}\right)}, \quad (22)$$

where $\Gamma_Z^{\ell\ell, \text{NP}}$ refers to the contribution induced by the sterile neutrinos.

In our study, we will also investigate the contributions of the sterile states to the width $\Gamma_Z^{\ell\ell, \text{NP}}$, or equivalently to the flavour conserving $\text{BR}(Z \rightarrow \ell^+ \ell^-)$, given by the diagonal contribution of Eq. (9), in order to address the possibility of violation of lepton flavour universality (LFU).

2.3 A high-luminosity Z -factory

Following the first evidence for a new (SM-like Higgs) bosonic resonance with a relatively low mass, the case for a high luminosity circular e^+e^- collider, operating at centre-of-mass energies ranging from the Z pole up to the top quark pair threshold is being actively studied [49]. These initial investigations are serving as a starting basis for a four-year design study of a ~ 100 km circumference e^+e^- collider, which defines the framework of the experimental prospects envisaged in this work. The baseline design of this machine assumes a layout similar to LEP/LHC with a number of equal-length arcs and long straight sections, in which the two beams must circulate in separate vacuum chambers, leading to $\mathcal{O}(10^4)$ bunches for an operation at the Z pole. These characteristics should allow to obtain a typical peak luminosity at the Z pole of $\sim 10^{36} \text{cm}^{-2} \text{s}^{-1}$. A year of operation at the Z pole centre-of-mass energy would then yield $\sim 10^{12}$ Z boson decays to be recorded. An alternative scheme, referred to as “crab-waist” scheme, could further increase the number of Z decays by an order of magnitude.

The LFV Z decays under scrutiny in this work imply a priori very clean experimental signatures. For instance, the decay $Z \rightarrow e^\pm \mu^\mp$ exhibits two and only two back-to-back oppositely charged leptons originating from a unique vertex. The decays $Z \rightarrow e^\pm (\mu^\pm) \tau^\mp$ could lead to somewhat more ambiguous final states, depending on the subsequent τ decays. They can actually proceed leptonically ($\text{BR}(\tau \rightarrow \ell \nu_\ell) \sim 17.5\%$) or hadronically, being dominated in the latter case by one- or three-prong decays. The direction of the τ particle is given by the momentum of the opposite lepton and hence can be used to kinematically constrain the decay. At least, experimental studies with a realistic detector simulation and the consideration of the relevant backgrounds are required to estimate the performance of the reconstruction of the decays involving τ leptons. In the following, we assume that the experimental reach for these LFV decays is fully driven by the accessible luminosity. We consider two bounds for the sensitivity: one $\sim \mathcal{O}(10^{-9})$ inspired by previous prospective studies at a Giga Z factory [50] (or for a Linear Collider) and another $\sim \mathcal{O}(10^{-13})$ corresponding to the highest foreseen luminosity scheme ($10^{13} Z$).

The parameter space of the models considered in this work is constrained in particular by the present electroweak precision measurements at the Z pole. The unprecedented statistics which could be obtained at FCC-ee are expected to improve significantly the determination of some of these key constraints. Other expected precision improvements concern observables also used in this work as is the case of the ratio of the partial widths of the Z decays into electrons and muons. The current precision on this ratio is at the level of 2.8×10^{-3} [51] and could be increased by two orders of magnitude, $\mathcal{O}(5 \times 10^{-5})$ [49]. The uncertainty of the partial decay width of $Z \rightarrow \tau^+ \tau^-$ must accordingly decrease. Moreover, the uncertainty on the invisible Z width (expressed as the number of light active neutrinos N_ν) should also decrease from 0.008 to 0.00004, by only a scaling of the uncertainty with the expected statistics. Nevertheless, the main systematic limitation comes from the luminosity measurement and must be accordingly evaluated. A reasonable target for the uncertainty on the number of neutrinos at FCC-ee is estimated at $\mathcal{O}(0.001)$ [49].

3 Constraints on sterile neutrino extensions of the SM

In order to account for neutrino masses and mixings, many extensions of the SM call upon the introduction of RH neutrinos (giving rise to a Dirac mass term for the neutral leptons) and/or other new particles. Their phenomenological impact can be important if the sterile states are not excessively heavy, and have sizeable mixings to the light (mostly active) neutrinos. For instance, this is the case of the ν MSM [38], the Inverse Seesaw (ISS) [39] and the low-scale type-I seesaw [52]. Many observables will be sensitive to the active-sterile mixings, and their current experimental values (or bounds) will thus constrain such SM extensions. In what follows we proceed to discuss the most relevant constraints on models with sterile fermions.

Neutrino oscillation data

The most important constraint on any model of massive neutrinos is to comply with ν -oscillation data [27–32]. In our analysis, we consider both normal and inverted hierarchies for the light neutrino spectrum [30]; the corresponding best-fit intervals in the case of normal hierarchy (NH) are

$$\begin{aligned} \sin^2 \theta_{12} &= 0.323, & \sin^2 \theta_{23} &= 0.567, & \sin^2 \theta_{13} &= 0.0234, \\ \Delta m_{21}^2 &= 7.60 \times 10^{-5} \text{eV}^2, & |\Delta m_{31}^2| &= 2.48 \times 10^{-3} \text{eV}^2, \end{aligned} \quad (23)$$

whereas for an inverted mass hierarchy (IH) the values are

$$\begin{aligned} \sin^2 \theta_{12} &= 0.323, & \sin^2 \theta_{23} &= 0.573, & \sin^2 \theta_{13} &= 0.024, \\ \Delta m_{21}^2 &= 7.60 \times 10^{-5} \text{eV}^2, & |\Delta m_{31}^2| &= 2.38 \times 10^{-3} \text{eV}^2. \end{aligned} \quad (24)$$

The value of the CP violating Dirac phase δ is still undetermined, although the complementarity of accelerator and reactor neutrino data starts reflecting in a better sensitivity to the CP violating phase δ [30,53] (and to the hierarchy of the light neutrino spectrum).

Unitarity constraints

The introduction of fermionic sterile states can give rise to non-standard neutrino interactions with matter. Bounds on the non-unitarity matrix η (cf. Eq.(6)), have been derived in [54,55] by means of an effective theory approach. We apply them in our numerical analysis for the cases in which the latter approach is valid, generically for sterile masses above the GeV, but below the electroweak scale, Λ_{EW} .

Electroweak precision data

Electroweak (EW) precision constraints on sterile fermions were firstly addressed in [56] with an effective approach (and therefore valid only for multi-TeV singlet states). The impact of sterile neutrinos on the invisible Z -decay width has also been addressed in [35, 57, 58], where it has been shown that $\Gamma(Z \rightarrow \nu\nu)$ can be reduced with respect to the SM prediction. Indeed, the addition of sterile states to the SM with a sizeable active-sterile mixing may have an impact on the electroweak precision observables either at tree-level (charged currents) or at higher order. In particular, the non-unitarity of the active neutrino mixing matrix, Eq. (6), implies that the couplings of the active neutrinos to the Z and W bosons are suppressed with respect to their SM values. Complying with LEP results on $\Gamma(Z \rightarrow \nu\nu)$ [48] will then also constrain these sterile neutrino extensions. In addition, we further require that the new contributions to the LFV Z decay width do not exceed the present uncertainty on the total Z width [48]: $\Gamma(Z \rightarrow \ell_1^\mp \ell_2^\pm) < \delta\Gamma_{\text{tot}}$.

LHC constraints

The presence of a new Higgs boson decay channel with (heavy) neutrinos in the final state can enlarge the total Higgs decay width, thus lowering the SM predicted decay branching ratios. LHC data already allows to constrain regimes where the sterile states are below the Higgs mass, due to the potential Higgs decays to an active and heavier (mostly) sterile neutrinos. In our analysis we apply the constraints derived in [59–61].

Leptonic and semileptonic meson decays

Further constraints arise from leptonic and semileptonic decays of pseudoscalar mesons K , D , D_s , B (see [62, 63] for kaon decays, [64, 65] for D and D_s decay rates, and [66, 67] for B -meson observations). These decays have been addressed in [34, 35] in the framework of the SM extended by sterile neutrinos, and it was found that the most severe bounds arise from the violation of lepton universality in leptonic kaon decays (parametrized by the observable Δr_K), which can receive important contributions from the new sterile states, due to the new phase space factors, and as a result of deviations from unitarity of the \tilde{U}_{PMNS} .

Laboratory searches

Negative searches for monochromatic lines in the spectrum of muons from $\pi^\pm \rightarrow \mu^\pm \nu$ decays [68, 69] also impose robust bounds on sterile neutrino masses in the MeV-GeV range.

Lepton flavour violation

Depending on the sterile neutrino mass regime, and on the active-sterile mixings, the new states will contribute to several charged lepton flavour violating processes such as $\ell \rightarrow \ell' \gamma$, $\ell \rightarrow \ell_1 \ell_2$ and $\mu - e$ conversion in muonic atoms. In our analysis we compute the contribution of the sterile states to all these observables [17, 42, 70–75], imposing compatibility with the bounds summarised in Table 1, also considering the impact of the future experimental sensitivities.

Neutrinoless double beta decay

The introduction of singlet neutrinos with Majorana masses allows for new processes like lepton number violating interactions, among which neutrinoless double beta decay remains the most important one [86]. In the SM extended by n_S sterile states, the effective neutrino mass m_{ee} is given by [87]:

$$m_{ee} \simeq \sum_{i=1}^{3+n_S} \mathbf{U}_{ei}^2 p^2 \frac{m_i}{p^2 - m_i^2} \simeq \left(\sum_{i=1}^3 \mathbf{U}_{ei}^2 m_{\nu_i} \right) + p^2 \left(\sum_{i=4}^{3+n_S} \mathbf{U}_{ei}^2 \frac{m_i}{p^2 - m_i^2} \right), \quad (25)$$

cLFV Process	Present Bound	Future Sensitivity
$\mu \rightarrow e\gamma$	5.7×10^{-13} [33]	6×10^{-14} [76]
$\tau \rightarrow e\gamma$	3.3×10^{-8} [77]	$\sim 3 \times 10^{-9}$ [78]
$\tau \rightarrow \mu\gamma$	4.4×10^{-8} [77]	$\sim 3 \times 10^{-9}$ [78]
$\mu \rightarrow eee$	1.0×10^{-12} [79]	$\sim 10^{-16}$ [80]
$\tau \rightarrow \mu\mu\mu$	2.1×10^{-8} [81]	$\sim 10^{-9}$ [78]
$\tau \rightarrow eee$	2.7×10^{-8} [81]	$\sim 10^{-9}$ [78]
$\mu^-, \text{Ti} \rightarrow e^-, \text{Ti}$	4.3×10^{-12} [82]	$\sim 10^{-18}$ [83]
$\mu^-, \text{Au} \rightarrow e^-, \text{Au}$	7×10^{-13} [84]	
$\mu^-, \text{Al} \rightarrow e^-, \text{Al}$		$10^{-15} - 10^{-18}$ [85]

Table 1: Current experimental bounds and future sensitivities for the low-energy cLFV observables considered in our study.

where $p^2 \simeq -(100 \text{ MeV})^2$ is an average estimate over different values depending on the decaying nucleus of the virtual momentum of the neutrino.

The neutrinoless double beta decay process is being actively searched for by several experiments, by means of the best performing detector techniques: among others, GERDA [88], EXO-200 [89,90], KamLAND-ZEN [91] have all set strong bounds on the effective mass, to which the amplitude of $0\nu 2\beta$ process is proportional. The sensitivities of current experiments put a limit on the effective neutrino Majorana mass - determining the amplitude of the neutrinoless double beta decay rate - in the range

$$|m_{ee}| \lesssim 140 \text{ meV} - 700 \text{ meV}. \quad (26)$$

In Table 2, we summarise the future sensitivity of ongoing and planned $0\nu 2\beta$ experiments.

Experiment	Ref.	$ m_{ee} $ (eV)
EXO-200 (4 yr)	[89, 90]	0.075 - 0.2
nEXO (5 yr)	[92]	0.012 - 0.029
nEXO (5 yr + 5 yr w/ Ba tagging)	[92]	0.005 - 0.011
KamLAND-Zen (300 kg, 3 yr)	[91]	0.045 - 0.11
GERDA phase II	[88]	0.09 - 0.29
CUORE (5 yr)	[93, 94]	0.051 - 0.133
SNO+	[95]	0.07 - 0.14
SuperNEMO	[96]	0.05 - 0.15
NEXT	[97, 98]	0.03 - 0.1
MAJORANA demo.	[99]	0.06 - 0.17

Table 2: Future sensitivity of several $0\nu 2\beta$ experiments.

In our analysis, we consider this observable using the most recent constraint from [90]; concerning the future sensitivity we take $|m_{ee}| \lesssim 0.01 \text{ eV}$.

Cosmological bounds

A number of cosmological observations [68,100] put severe constraints on sterile neutrinos with a mass below the TeV. While CMB analysis with the Planck satellite disfavour very light sterile neutrinos (with a mass $\lesssim \text{eV}$) [14], a $\sim \text{keV}$ sterile neutrino may instead be a viable DM candidate, also offering a possible explanation for the observed X-ray line in galaxy clusters spectra at an

energy ~ 3.5 keV [101, 102] and for the origin of pulsar kicks, or even to the baryon asymmetry of the Universe (for a review see [103]).

The cosmological bounds are in general derived by assuming the minimal possible abundance (in agreement with neutrino oscillations) of sterile neutrinos in halos consistent with standard cosmology. However, the possibility of a non-standard cosmology with a very low reheating temperature or a scenario where the sterile neutrinos couple to a dark sector [104], could allow to evade some of the above bounds, as argued in [105]. In this analysis, aiming at being conservative, we will allow for the violation of these cosmological bounds in some scenarios, explicitly stating it.

4 A minimal “3+1 toy model”

The most simple approach to studying the phenomenological impact of sterile fermions lies in considering a minimal model, where one extra sterile Majorana state is added to the three light active neutrinos of the SM.

4.1 The “3+1” framework

In the present framework, no assumption is made on the underlying mechanism of neutrino mass generation. In addition to the three (light) active masses and corresponding mixing angles, it is only assumed that the leptonic sector contains extra degrees of freedom: the mass of the new sterile state, m_4 , three active-sterile mixing angles θ_{i4} , two new (Dirac) CP phases and one extra Majorana phase. This leads to the definition of a 4×4 mixing matrix \mathbf{U}_{ij} , whose 3×4 sub-matrix \mathbf{U}_{lj} appears in Eq. (5).

Although the experimental and observational constraints mentioned in Section 3 put no upper limit on the mass of the heavy neutrino, we notice however that the decay of the (mostly) sterile heavy states should comply with the perturbative unitary condition [106–111],

$$\frac{\Gamma_{\nu_i}}{m_{\nu_i}} < \frac{1}{2} \quad (i \geq 4). \quad (27)$$

Assuming that the sterile mass is indeed sufficiently large to allow for its 2-body decay into a W^\pm boson and a charged lepton, or into a light (active) neutrino and either a Z or a Higgs boson, the total decay width of such a state ($i \geq 4$) is given by

$$\Gamma_{\nu_i} = \sum_{j=1}^3 [\Gamma(\nu_i \rightarrow \ell_j W) + \Gamma(\nu_i \rightarrow \nu_j Z) + \Gamma(\nu_i \rightarrow \nu_j H)] \approx \frac{\alpha_w}{4 M_W^2} \mathbf{C}_{ii}, \quad (28)$$

where $\alpha_w = g_w^2/4\pi$, and \mathbf{C}_{ii} as given in Eq. (8). Since the dominant contribution arises from the charged current term, one is led to the following bound on the sterile masses and their couplings to the active states [106–111]:

$$m_{\nu_i}^2 \mathbf{C}_{ii} < 2 \frac{M_W^2}{\alpha_w} \quad (i \geq 4). \quad (29)$$

In our analysis, and for both NH and IH light neutrino spectra, we scan over the following range for the sterile neutrino mass

$$10^{-9} \text{ GeV} \lesssim m_4 \lesssim 10^6 \text{ GeV} , \quad (30)$$

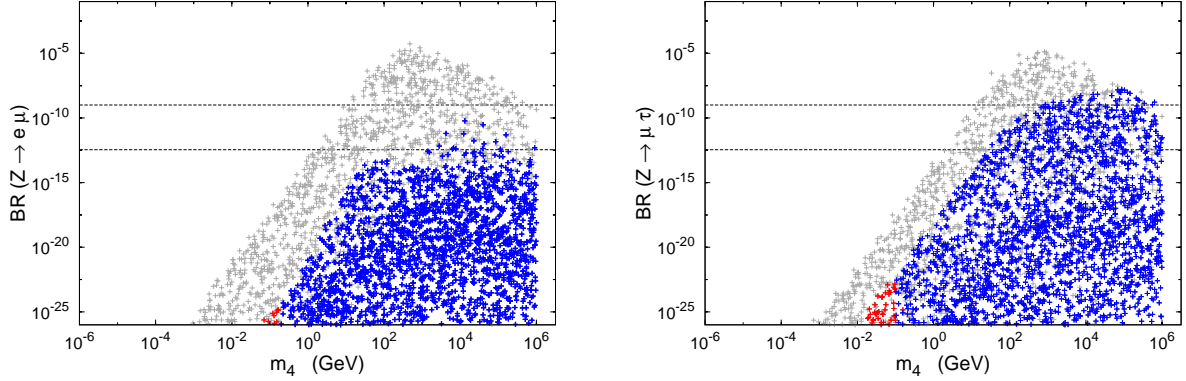


Figure 2: The “3+1 model”: on the left $\text{BR}(Z \rightarrow e\mu)$ and on the right $\text{BR}(Z \rightarrow \mu\tau)$, as a function of the mass of the (mostly) sterile state, m_4 , for a NH light neutrino spectrum. Blue points are in agreement with cosmological bounds, while the red ones would require considering a non-standard cosmology. In grey we denote points already excluded by other (non-cosmological) bounds (see text for a description). The upper horizontal dashed line corresponds to the expected sensitivity for a GigaZ facility as a Linear Collider, $\mathcal{O}(10^{-9})$, the lower one to the FCC-ee $\sim \mathcal{O}(10^{-13})$.

while the active-sterile mixing angles are randomly varied in the interval $[0, 2\pi]$, always ensuring that the condition of Eq. (29) is respected. All CP phases are also taken into account, and likewise randomly varied between 0 and 2π .

4.2 LFU violation: $Z \rightarrow \ell\ell$ decays in the “3+1 model”

We begin by addressing the contributions of the additional sterile state to the violation of flavour universality, considering the observable ΔR_Z^{lep} , introduced in Eq. (22). Although one could have a non-negligible violation of LFU $\sim \mathcal{O}(10^{-3})$, a number of experimental bounds (LFV constraints, complying with U_{PMNS} data, ...) preclude this possibility, and one has at most $\Delta R_Z^{\text{lep}} \lesssim 10^{-10}$, clearly beyond experimental sensitivity.

4.3 LFV Z decays in the “3+1 model”

We proceed to discuss the impact of the additional sterile state regarding lepton flavour violating Z decays. In Fig. 2 we illustrate our results regarding the observation of $\text{BR}(Z \rightarrow e\mu)$ and $\text{BR}(Z \rightarrow \mu\tau)$ at a future high-luminosity Z -factory, considering a NH light neutrino spectrum (the results for an IH spectrum do not exhibit any significant qualitative nor quantitative difference in what concerns the branching fractions, and so we will not display them here). As already mentioned in Section 3, we identify in red the points that are typically disfavoured from standard cosmology arguments. Grey points denote failure to comply with (at least) one of the following constraints: ν -oscillation data, bounds on the U_{PMNS} matrix, bounds from EW precision data, LHC bounds, laboratory bounds, constraints from rare leptonic meson decays; conflict with bounds from cLFV decays, neutrinoless double beta decays or Z -boson decay width data (invisible and lepton flavour conserving). Blue points are in agreement with *all* imposed constraints.

As can be seen from Fig. 2, such a minimal extension of the SM can indeed account⁴ for values of $\text{BR}(Z \rightarrow \ell_1^\mp \ell_2^\pm)$ within the sensitivity of a high luminosity Z -factory, such as the FCC-ee. (We notice that we have only displayed here values of the (mostly) sterile state mass $m_4 \gtrsim 10^{-3}$ GeV, since smaller values are associated to $\text{BR}(Z \rightarrow \ell_1^\mp \ell_2^\pm) \lesssim 10^{-28}$).

Despite the potential of this simple “toy-model” to account for significant LFV Z decay branching fractions (which could be as large as $\mathcal{O}(10^{-6})$), these cannot be reconciled with current bounds on low-energy cLFV processes (see Table 1), to which the sterile states also contribute. While the recent MEG bound on $\mu \rightarrow e\gamma$ decays excludes important regions of the parameter space⁵, the contribution of the Z penguin diagrams to cLFV 3-body decays and $\mu - e$ conversion in nuclei severely constrains the flavour violating $Z\ell_1^\mp \ell_2^\pm$ vertex (see also [18–20]). This is especially manifest in the case of $Z \rightarrow e\mu$ decays, since the severe constraints from $\text{BR}(\mu \rightarrow 3e)$ and $\text{CR}(\mu - e, \text{Au})$ typically preclude $\text{BR}(Z \rightarrow e\mu) \gtrsim 10^{-13}$; however, and for a regime of very heavy sterile states ($m_4 \gtrsim 10^4$ GeV), the “3+1 model” can nevertheless account for $\text{BR}(Z \rightarrow e\mu)$ within FCC-ee reach.

The comparatively less stringent bounds for cLFV in the $\mu - \tau$ sector allow for larger $\text{BR}(Z \rightarrow \mu\tau)$: values above $\mathcal{O}(10^{-13})$ can be found for $m_4 \gtrsim 50$ GeV, and even larger branching fractions, $\mathcal{O}(10^{-8})$ (within reach of a GigaZ facility as a Linear Collider) for $m_4 \gtrsim 500$ GeV. Although not displayed here, the predictions of the “3+1 model” for the $\text{BR}(Z \rightarrow e\tau)$ exhibit a similar behaviour to what is observed for $Z \rightarrow \mu\tau$ decays.

The rôle of the different mixing angles is displayed in Fig. 3, where we present $\text{BR}(Z \rightarrow e\mu)$ and $\text{BR}(Z \rightarrow \mu\tau)$, respectively as a function of the active-sterile mixing angles, θ_{14} and θ_{34} . For completeness, we single out in these plots another observable, which is the effective neutrino mass in neutrinoless double beta decays given in Eq. (25). Dark yellow regions correspond to values of $|m_{ee}|$ within future sensitivity, i.e. $0.01 \text{ eV} \lesssim |m_{ee}| \lesssim 0.1 \text{ eV}$ (see Table 2).

As can be verified from Fig. 3, the maximal values of $\text{BR}(Z \rightarrow \ell_1^\mp \ell_2^\pm)$ are associated with larger values of the active-sterile mixing angle. (In each panel, the more dense “diagonal” band corresponds to contributions arising from configurations where the active-sterile mixing angle depicted in the x -axis is much larger than the other two.) As visible in the left panel of Fig. 3, for a regime of large θ_{14} , one can be indeed within reach of near future $0\nu 2\beta$ decay dedicated experiments (in agreement with the findings of [36]). However, the associated $\text{BR}(Z \rightarrow e\mu)$ lies beyond FCC-ee expected sensitivity. Although this region would indeed be larger in the case of an IH for the light neutrino spectrum, the corresponding $\text{BR}(Z \rightarrow e\mu)$ would still remain below 10^{-13} .

The prospects regarding the observation of a $Z \rightarrow \ell_1^\mp \ell_2^\pm$ decay at a high-luminosity Z -factory for the full sterile neutrino parameter space studied in our analysis are summarised in Fig. 4, where we display the $(\sin^2 \theta_{i4}, m_4)$ plane. (We notice that in agreement with Eq. (29) the upper regions, corresponding to a regime of heavy masses and large active-sterile mixings, are precluded due to perturbativity arguments.)

As can be confirmed, and in agreement with the previous discussion, the largest values of the lepton flavour violation Z -decays correspond to regimes of large sterile masses, in association with sizeable mixing angles. The $(\sin^2 \theta_{14}, m_4)$ parameter space is strongly constrained by the current bounds from $\text{BR}(\mu \rightarrow 3e)$ - as would be the case of $(\sin^2 \theta_{24}, m_4)$, not displayed here - and from $\text{CR}(\mu - e, \text{Au})$, while $\sin^2 \theta_{34} \gtrsim 10^{-4}$ are excluded due to constraints arising from $\text{BR}(\tau \rightarrow 3\mu)$.

⁴In addition to being experimentally ruled out, we notice that very large branching fractions, associated with a regime of masses above the TeV, would be precluded due to the perturbativity bound of Eq. (29), which significantly constraints the sterile-active mixings for heavy sterile states.

⁵The flavour violating $Z\ell_1^\mp \ell_2^\pm$ vertex might induce higher order (2-loop) contributions to radiative muon decays [19]; however, in the present study, we do not take such contributions into account.

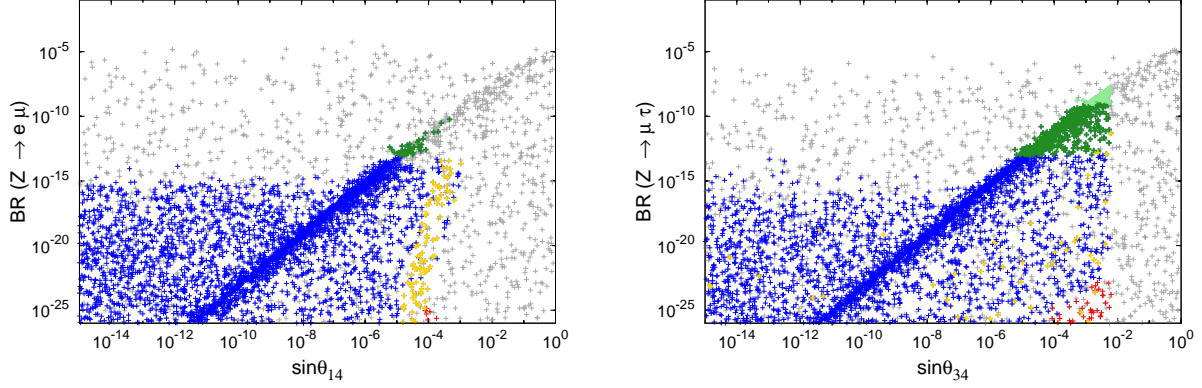


Figure 3: The “3+1 model”: $\text{BR}(Z \rightarrow e\mu)$ as a function of the active-sterile mixing θ_{14} (left) and $\text{BR}(Z \rightarrow \mu\tau)$ as a function of θ_{34} (right) for a NH light neutrino spectrum. Blue points are in agreement with cosmological bounds, while the red ones would require considering a non-standard cosmology. In grey we denote points already excluded by other (non-cosmological) bounds (see text for a description); dark-yellow points denote an associated $|m_{ee}|$ within experimental reach (i.e. $0.01 \text{ eV} \lesssim |m_{ee}| \lesssim 0.1 \text{ eV}$). Dark green points are associated with $10^{-13} \lesssim \text{BR}(Z \rightarrow \ell_1^\mp \ell_2^\pm) \lesssim 10^{-9}$, while light green ones correspond to $\text{BR}(Z \rightarrow \ell_1^\mp \ell_2^\pm) \gtrsim 10^{-9}$.

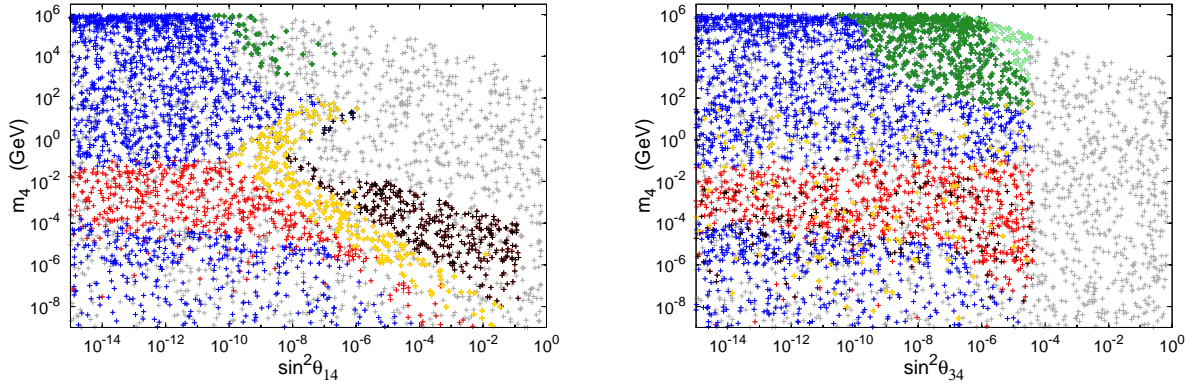


Figure 4: The “3+1 model”: on the left $(\sin^2 \theta_{14}, m_4)$ parameter space of the sterile state, displaying the regimes for $\text{BR}(Z \rightarrow e\mu)$ for a NH light neutrino spectrum. Line and colour code as in Fig. 3 (dark green points are associated with $10^{-13} \lesssim \text{BR}(Z \rightarrow e\mu) \lesssim 10^{-9}$, while light green ones correspond to $\text{BR}(Z \rightarrow e\mu) \gtrsim 10^{-9}$). On the right, $(\sin^2 \theta_{34}, m_4)$ displaying with the same colour code the corresponding regimes for $\text{BR}(Z \rightarrow \mu\tau)$.

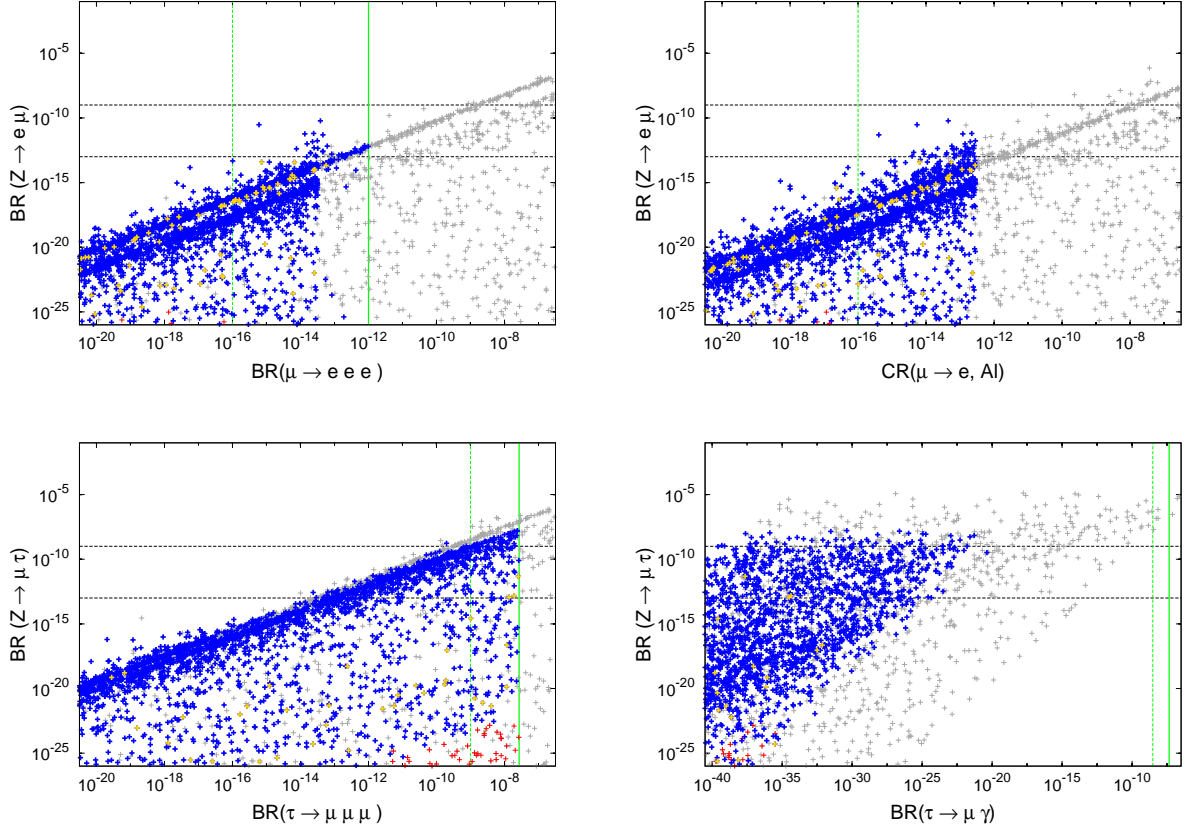


Figure 5: The “3+1 model”: on the upper panels $\text{BR}(Z \rightarrow e\mu)$ versus $\text{BR}(\mu \rightarrow 3e)$ (left) and $\text{CR}(\mu - e, \text{Al})$ (right), on the lower panels $\text{BR}(Z \rightarrow \mu\tau)$ versus $\text{BR}(\tau \rightarrow 3\mu)$ (left) and $\text{BR}(\tau \rightarrow \mu\gamma)$ (right) for a NH light neutrino spectrum. Line and colour code as in Fig. 2. When present, the additional green vertical lines denote the current bounds (solid) and future sensitivity (dashed), and dark-yellow points denote an associated $|m_{ee}|$ within experimental reach.

We conclude the analysis of the “3+1 model” by investigating the complementary rôle of a high-luminosity Z -factory with respect to low-energy (high-intensity) cLFV dedicated experiments. From the above discussion, it is clear that low-energy cLFV processes play a constraining rôle in the maximal values of $\text{BR}(Z \rightarrow \ell_1^\mp \ell_2^\pm)$; we now explore which facility has the greater potential to probe cLFV in the “3+1 model”. This is illustrated in Fig. 5, where we display the sterile neutrino contributions to $\text{BR}(Z \rightarrow \ell_1^\mp \ell_2^\pm)$ versus different low-energy cLFV observables.

As can be inferred from the upper panels of Fig. 5, low-energy cLFV dedicated facilities offer much better prospects to probe lepton flavour violation in the $\mu - e$ sector of the “3+1 model” than a high-luminosity Z -factory. In particular, Mu3e (PSI) [80] and COMET (J-PARC) [85] will be sensitive to regions in parameter space associated with $\text{BR}(Z \rightarrow e\mu) \sim 10^{-17 \div -13}$, beyond the reach of FCC-ee. Interestingly, the situation is reversed for the case of the $\mu - \tau$ sector: as can be seen from both lower panels of Fig. 5, a high-luminosity Z -factory such as FCC-ee allows to probe much larger regions of the “3+1 model” than low-energy facilities (searching for radiative and 3-body τ decays). In particular, we draw the attention to a small subset of the parameter space, which can be simultaneously probed via $Z \rightarrow \mu\tau$ and $\tau \rightarrow 3\mu$ decays, and which is also

within reach of near future $0\nu 2\beta$ decay searches (especially in the case of an IH light neutrino spectrum, not displayed here), opening the door for a three-fold experimental test of this minimal SM extension.

5 The neutrino minimal SM: ν MSM

The ν MSM consists in a truly minimal extension of the SM via the inclusion of three RH neutrinos, aiming at simultaneously addressing the problems of neutrino mass generation, the baryon asymmetry of the Universe (BAU) and providing a viable DM candidate [38, 112–114]. In its most successful realisations, the thermally produced lightest sterile state accounts for the DM relic density, while the two heavier states generate the masses of the active neutrinos. The CP violating oscillations of the latter states produce a lepton asymmetry via flavoured leptogenesis [115], which is converted into a baryon asymmetry. (For a detailed discussion, see [38, 112].) More relaxed ν MSM realisations forego a full (or partial) explanation of the DM relic density.

5.1 Sterile neutrinos in the ν MSM

The addition of three generations of RH Majorana states ν_R to the SM particle content allows to add the following terms to the leptonic Lagrangian:

$$\mathcal{L}_{\text{mass}}^{\nu\text{MSM}} = -Y_{ij}^\nu \bar{\nu}_{Ri} \tilde{H}^\dagger L_j - \frac{1}{2} \bar{\nu}_{Ri} M_{Mij} \nu_{Rj}^c + \text{H.c.}, \quad (31)$$

where $i, j = 1, 2, 3$ are generation indices, L is the $\text{SU}(2)_L$ lepton doublet and $\tilde{H} = i\sigma_2 H^*$; Y^ν denotes the Yukawa couplings, while M_M is a Majorana mass matrix (leading to the violation of total lepton number, $\Delta L = 2$). After EW symmetry breaking, the neutral lepton spectrum is composed of six Majorana fermions: the active (mostly left-handed) light states, and three heavier sterile neutrinos. The light neutrino masses, $m_{\nu_{1-3}}$ are given by a type I seesaw relation⁶,

$$m_{\nu_{1-3}} = -m_D^T (M_M)^{-1} m_D, \quad \text{where} \quad m_D = Y^\nu v, \quad (32)$$

with $v = 174$ GeV the Higgs vacuum expectation value. The heavier spectrum, corresponding to $m_{\nu_{4-6}}$ is given by [114]

$$m_{\nu_{4-6}} = M_M + \frac{1}{2} \left(\frac{1}{M_M} (m_D^* m_D^T) + (m_D^* m_D^T)^* \frac{1}{M_M} \right) \quad (33)$$

where corrections of second order in m_D/M_M are taken into account.

In order to be a good DM candidate, the couplings of ν_4 to the other active and sterile states must be very small. This translates into associated tiny Yukawa couplings, and negligible mixings with the heavier steriles, ν_5 and ν_6 . In addition to light neutrino mass generation (in which ν_4 plays no rôle), the latter two states, are responsible for generating lepton asymmetries: on the one hand, the asymmetries produced at early times will give rise to BAU, while those at late times can account for the correct rate of thermal ν_4 production [116]. In both cases, the leptonic asymmetry generation in general relies on a resonant amplification [117], and the heavier steriles, ν_5 and ν_6 , exhibit a certain amount of degeneracy.

⁶Despite the comparatively low seesaw scale of the ν MSM, working in the seesaw limit, i.e. $m_D/M_M \ll 1$ is still a valid approximation.

There are several possible parametrizations of the physical ν MSM degrees of freedom. Drawing from the analysis of the “3+1 model” discussed in Section 4, we prefer to carry our discussion in terms of the six mass eigenvalues, while encoding all physical mixing angles and CP violating phases (Dirac and Majorana) in an effective 6×6 unitary mixing matrix, \mathbf{U} , as it allows to readily implement the already well-established bounds on the ν MSM parameter space. The angles θ_{lj} , $l = 1, 2, 3$, $j = 4, 5, 6$ encode the active-sterile mixings, while the mixings between the sterile states are given by three additional angles $\theta_{45,46,56}$. The matrix \mathbf{U} is further parametrized by 3 additional Majorana and 9 Dirac phases. The heavier masses can be written as:

$$m_j = \text{diag}(m_{\text{DM}}, M - \delta_M, M + \delta_M) \quad (34)$$

with $j = 4, 5, 6$. In the above $m_4 = m_{\text{DM}}$ is the mass of the DM candidate.

In addition to the general constraints on sterile neutrino extensions of the SM, the peculiar features of the ν MSM (generation of the BAU and a viable DM candidate) lead to a very constrained parameter space. Here we rely on the results of [114], where the most relevant constraints are translated into bounds on the (U^2, M) planes, as well as on the splitting δ_M , which is of the order $\sim 10^{-4}$ eV – 1 keV. The quantity U^2 encodes the experimentally relevant combination of couplings; in the limit of small active-sterile mixings, and in analogy to [114], we will use

$$\begin{aligned} U_4^2 &= U_{e4}^2 + U_{\mu4}^2 + U_{\tau4}^2 = \sum_l \sin^2 \theta_{l4}, \\ U_{4-6}^2 &= \sum_l \sin^2 \theta_{l4} + \sin^2 \theta_{l5} + \sin^2 \theta_{l6}, \quad \text{with } l = e, \mu, \tau. \end{aligned} \quad (35)$$

Dark matter constraints

As reported in [114], observations of the matter distribution in the Universe constrain the DM free streaming length; realistic scenarios (including combinations of X-ray bounds and Ly_α forest reconstruction, among others) suggest $10 \text{ keV} \lesssim m_4 \lesssim 50 \text{ keV}$; combining the latter bounds with a successful production of the required DM abundance, one is led to bounds on the corresponding mixing angles, $\theta_{l4}^2 \sim \mathcal{O}(10^{-13} - 10^{-8})$, $l = 1, 2, 3$. In our analysis we will not exclude regions in which the lightest sterile would have a relic density below the observed value (i.e., smaller values of θ_{l4}^2).

Heavy sterile parameter space

As discussed in [114], the allowed (U_{4-6}^2, M) plane corresponds to a well-defined region: the regime of very small mixings is excluded by the impossibility of correctly reproducing the active neutrino mass differences (seesaw exclusion), while larger mixings preclude the generation of a baryon asymmetry from RH neutrino oscillations; the BAU exclusion surface extends to the seesaw exclusion, effectively constraining the average $\nu_{5,6}$ masses to lie below the EW scale. Finally, the small mass regime (i.e., $m_{\nu_{5,6}} \lesssim 0.1 \text{ GeV}$) is also ruled out due to conflict with BBN bounds and direct searches (at PS191 [118, 119]). Although we have used the BAU-derived constraints on the magnitude of the distinct mixing angles, we have not attempted at doing the same for the CP violating phases, which for simplicity were set to zero in this analysis.

In Fig. 6, and for completeness, we summarise the ν MSM parameter space investigated in our analysis, closely following the dedicated studies of [114], and assuming a NH for the light neutrino spectrum.

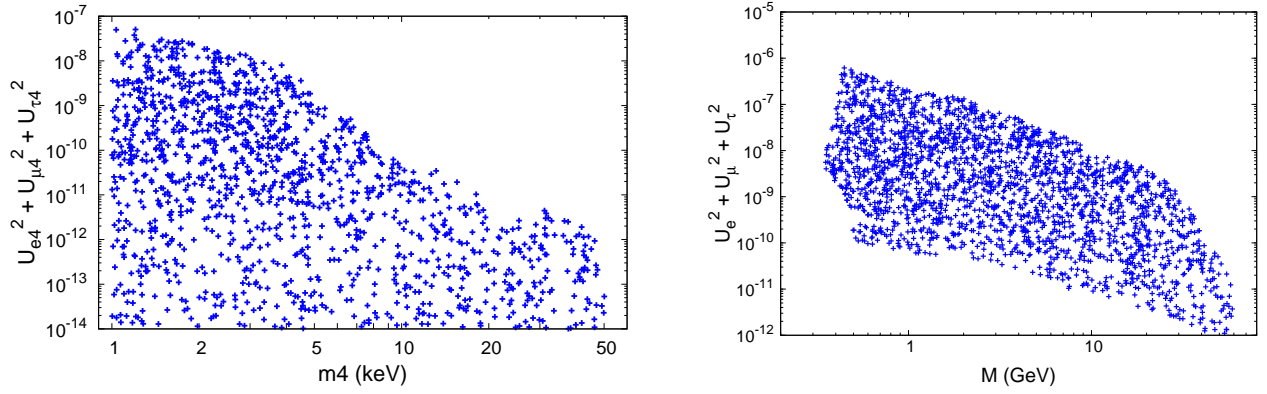


Figure 6: ν MSM model: (U_4^2, m_{DM}) and (U_{4-6}^2, M) parameter spaces (as identified in [114]), respectively on the left and right panels, for a NH light neutrino spectrum.

5.2 Leptonic Z decays in the ν MSM

We begin by discussing the expected $\text{BR}(Z \rightarrow \ell_1^\mp \ell_2^\pm)$ within the ν MSM. In Fig. 7, we display the range of LFV Z boson decays across the allowed parameter space.

As expected from the results of Section 4, the maximal values of $\text{BR}(Z \rightarrow \ell_1^\mp \ell_2^\pm)$ occur for a regime where sizable RH neutrino masses are accompanied by the maximally allowed active-sterile mixings. Nevertheless, and as can be directly inferred from the left panel of Fig. 7, one can have, at best, $\text{BR}(Z \rightarrow \ell_1^\mp \ell_2^\pm) \lesssim \mathcal{O}(10^{-16})$. Larger values would indeed be possible, but are excluded by the requirement of generating the observed BAU. A clearer insight can be drawn from the right panel of Fig. 7, where one verifies that, for instance, $\text{BR}(Z \rightarrow e\mu) \lesssim \mathcal{O}(10^{-16})$. Similar ranges are obtained for the other LFV final states. Although we do not display the corresponding analysis here, we have numerically verified that similar results are obtained for a IH light neutrino spectrum. We also notice that the ranges for the LFV Z -decays BRs are in fair agreement⁷ with the analysis carried for the truly minimal “3+1 model” in Section 4, considering the appropriate mass and sterile mixing regime.

Regarding the departure from unitarity of the \tilde{U}_{PMNS} matrix in the surveyed parameter space, we notice that (as expected) it is comparatively small: $\tilde{\eta} \lesssim 10^{-6}$. In what concerns low-energy (charged) lepton flavour observables, due to the smallness of the active-sterile mixings, the contributions are typically very small, as already suggested in [120] regarding $\mu - e$ conversion in Nuclei. Finally, and concerning the violation of lepton universality in Z -decays, the contributions of the new sterile states of the ν MSM are truly negligible.

For completeness, we summarise in Table 3 two examples of points in the ν MSM parameter space that would account for “maximal” values of $\text{BR}(Z \rightarrow \ell_1^\mp \ell_2^\pm)$.

It has been recently pointed out that high-luminosity Z -factories (such as FCC-ee) offer a promising set-up for direct searches of RH (nearly) sterile neutrinos, as those present in the

⁷It is worth mentioning that our study of the ν MSM - based on a “3+3” analysis along the lines of the “3+1 toy model” - leads to a conservative estimate of the corresponding $\text{BR}(Z \rightarrow \ell_1^\mp \ell_2^\pm)$. The effective 6×6 unitary mixing matrix whose entries are thus scanned allows to cover, and even go beyond, regions of parameter space strictly arising in the type-I seesaw of the ν MSM. Hence, we are not under-estimating the cLFV Z decays.

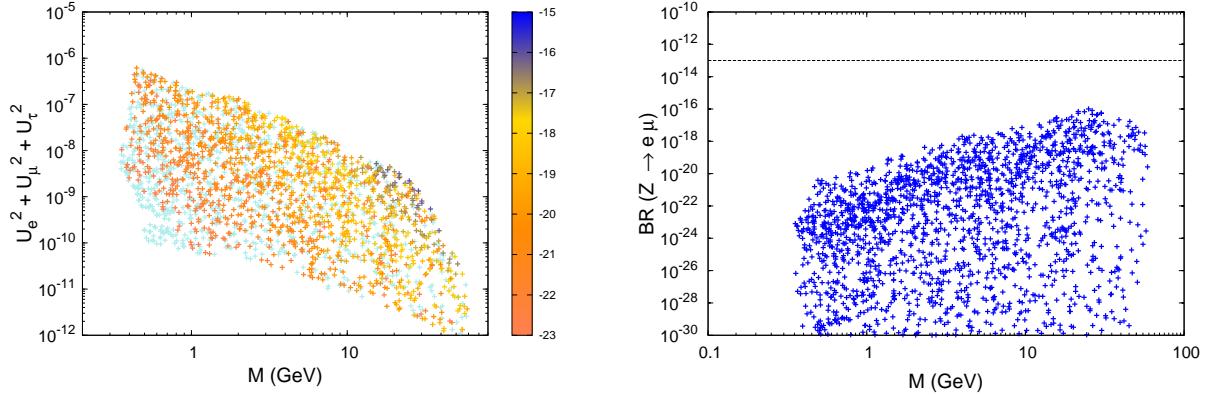


Figure 7: ν MSM model: on the left, maximal values of $\text{BR}(Z \rightarrow \ell_1^\mp \ell_2^\pm)$ on the (U_{4-6}^2, M) parameter space, from larger (dark blue) to smaller (orange) values. Cyan denotes values of the branching fraction below 10^{-23} . On the right $\text{BR}(Z \rightarrow e\mu)$ as a function of M , for the points in the allowed (U_{4-6}^2, M) parameter space. Both cases correspond to a NH light neutrino spectrum.

m_4 (keV)	M (GeV)	U_4^2	U_{4-6}^2	$\text{BR}(Z \rightarrow e\mu)$	$\text{BR}(Z \rightarrow \mu\tau)$	$\text{BR}(Z \rightarrow e\tau)$
11.8	26.2	4×10^{-25}	1.8×10^{-9}	10^{-16}	7×10^{-18}	2×10^{-21}
1.1	34.4	1.3×10^{-16}	5.4×10^{-10}	3×10^{-25}	2×10^{-17}	8×10^{-17}

Table 3: Example of two points in ν MSM parameter space with associated $\text{BR}(Z \rightarrow \ell_1^\mp \ell_2^\pm) \gtrsim 10^{-17}$.

framework of the ν MSM [37]. The small active-sterile mixing angles lead to long lifetimes, with decay lengths comprised between 100 microns and 5m; this would allow to cover a large region of the phase-space for heavy neutrino masses between 10 and 80 GeV, reaching down to a mixing as small as $U_{4-6}^2 \approx 10^{-12}$ (thus complementing [37] the probing power of the SHIP experiment [121]). Lepton flavour violating Z decays do not allow a further synergy with the above mentioned searches for light RH neutrinos, as those present in the ν MSM. However, the observation of LFV Z decays at a high-luminosity Z -factory would suggest that sources of LFV - other than the ν MSM - are present. Conversely, the interpretation of displaced vertices in association of a long-lived RH state of the ν MSM should not be accompanied by a $\text{BR}(Z \rightarrow \ell_1^\mp \ell_2^\pm)$ within FCC-ee sensitivity.

6 The Inverse Seesaw scenario

The Inverse Seesaw mechanism [39] consists in an appealing extension of the SM via RH and sterile neutrinos. Contrary to most (type I) low-energy seesaw realisations, the ISS allows to accommodate neutrino data with natural values of the Yukawa couplings for a comparatively low seesaw scale. The possibility of having sizeable mixings between the active and sterile states renders the model phenomenologically rich, with a potential impact for a number of observables.

Depending on its actual realisation, the ISS does allow to accommodate the observed DM relic abundance and (potential) indirect DM detection hints [122, 123].

6.1 The (3,3) ISS realisation

In the ISS, $n_R \geq 2$ generations of RH neutrinos ν_R and n_X generations of extra $SU(2)$ singlets fermions X (such that $n_R + n_X = n_s$), are added to the SM content. Both ν_R and X carry lepton number $L = +1$ [39]. Here we consider a specific ISS realisation in which $n_R = n_X = 3$, the so-called (3,3) realisation. The SM Lagrangian is thus extended as

$$\mathcal{L}_{\text{ISS}} = \mathcal{L}_{\text{SM}} - Y_{ij}^\nu \bar{\nu}_{Ri} \tilde{H}^\dagger L_j - M_{Rij} \bar{\nu}_{Ri} X_j - \frac{1}{2} \mu_{Xij} \bar{X}_i^c X_j + \text{h.c.}, \quad (36)$$

where $i, j = 1, 2, 3$ are generation indices and $\tilde{H} = i\sigma_2 H^*$. Notice that $U(1)_L$ (i.e., lepton number) is broken only by the non-zero Majorana mass term μ_X , while the Dirac-type RH neutrino mass term M_R does conserve lepton number. In the $(\nu_L, \nu_R^c, X)^T$ basis, and after EW symmetry breaking, the (symmetric) 9×9 neutrino mass matrix \mathcal{M} is given by

$$\mathcal{M} = \begin{pmatrix} 0 & m_D^T & 0 \\ m_D & 0 & M_R \\ 0 & M_R^T & \mu_X \end{pmatrix}, \quad (37)$$

with $m_D = Y^\nu v$ the Dirac mass term, v being the vacuum expectation value of the SM Higgs boson. Under the assumption that $\mu_X \ll m_D \ll M_R$, the diagonalization of \mathcal{M} leads to an effective Majorana mass matrix for the active (light) neutrinos [124],

$$m_\nu \simeq m_D^T M_R^{T-1} \mu_X M_R^{-1} m_D. \quad (38)$$

The remaining (mostly) sterile states form nearly degenerate pseudo-Dirac pairs, with masses

$$m_{S\pm} = \pm \sqrt{M_R^2 + m_D^2} + \frac{M_R^2 \mu_X}{2(m_D^2 + M_R^2)}. \quad (39)$$

It proves convenient to introduce the following matrix $M = M_R \mu_X^{-1} M_R^T$, which is diagonalized as $D M D^T = \hat{M}$. The eigenvalues of M are thus the entries of the diagonal matrix \hat{M} . In order to write the neutrino Yukawa couplings, it is useful to use a generalization of the Casas-Ibarra parametrization [125], which allows to cast Y^ν as

$$Y^\nu = \frac{1}{v} D^\dagger \sqrt{\hat{M}} R \sqrt{\hat{m}_\nu} U_{\text{PMNS}}^\dagger. \quad (40)$$

In the above, $\sqrt{\hat{m}_\nu}$ is a diagonal matrix containing the square roots of the three light neutrino mass eigenvalues m_ν , R is an arbitrary 3×3 complex orthogonal matrix, parametrized by 3 complex angles, encoding the remaining degrees of freedom. (Without loss of generality, one can choose to work in a basis where M_R is a real diagonal matrix, as are the charged lepton Yukawa couplings.) The full neutrino mass matrix is then diagonalized by the 9×9 unitary mixing matrix \mathbf{U} as $\mathbf{U}^T \mathcal{M} \mathbf{U} = \text{diag}(m_i)$. In the basis where the charged lepton mass matrix is diagonal, the leptonic mixing matrix is given by the rectangular 3×9 sub-matrix corresponding to the first three columns of \mathbf{U} , with the 3×3 block corresponding to the (non-unitary⁸) \tilde{U}_{PMNS} .

In the following numerical study, the contributions to the distinct observables are derived through the following general scan: leading to the construction of the 9×9 mass matrix in Eq. (37), the modulus of the entries of the matrices M_R and μ_X are randomly taken to lie on the

⁸For further studies on non-unitarity effects in the Inverse Seesaw see, for instance, [126–128].

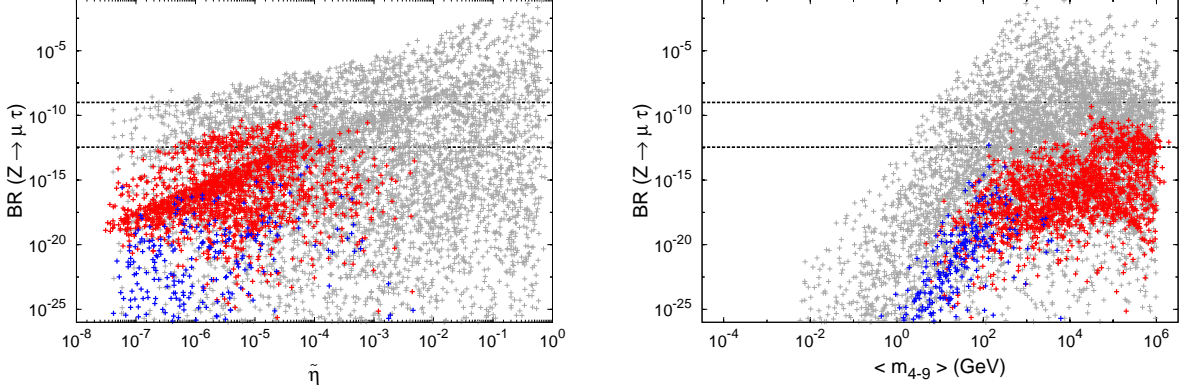


Figure 8: ISS realisation: $\text{BR}(Z \rightarrow \mu\tau)$ as a function of $\tilde{\eta}$ (left) and of the average value of the mostly sterile state masses (right), $\langle m_{4-9} \rangle$, for a NH light neutrino spectrum. Line and colour code as in Fig. 2.

intervals $0.1 \text{ MeV} \lesssim (M_R)_i \lesssim 10^6 \text{ GeV}$ and $0.01 \text{ eV} \lesssim (\mu_X)_{ij} \lesssim 1 \text{ MeV}$, with complex entries for the lepton number violating matrix μ_X ; we also take complex angles for the R matrix, randomly varying their values in the interval $[0, 2\pi]$. The modified Casas-Ibarra parametrization for Y^ν , Eq. (40), ensures that constraints from neutrino oscillation data are satisfied.

6.2 ISS: Violation of flavour universality in Z decays

Despite the contributions of the several additional states of the ISS to the violation of lepton flavour universality observable ΔR_Z^{lep} , see Eq. (22), the ISS also remains short of the future sensitivity. Although in regions of the surveyed parameter space one could in principle have $\Delta R_Z^{\text{lep}} \sim 10^{-3}$, this regions are experimentally excluded, as there are strong conflicts with numerous bounds, especially those arising from low-energy cLFV observables.

6.3 LFV Z decays in the ISS

We first consider the LFV decays $Z \rightarrow \mu\tau$, displaying the corresponding BRs on Fig. 8 as a function of $\tilde{\eta}$ (see Eq. (7)), and as a function of the average of the absolute masses of the mostly sterile states,

$$\langle m_{4-9} \rangle = \sum_{i=4\dots 9} \frac{1}{6} |m_i|. \quad (41)$$

The results collected in Fig. 8 reveal that the present ISS realisation can account for sizeable values of LFV Z -decay branching ratios: this in general requires the presence of sterile states with a mass $\gtrsim \Lambda_{\text{EW}}$, and can occur even for very mild deviations from unitarity of the \tilde{U}_{PMNS} . Other LFV decays, $Z \rightarrow e\mu$ and $Z \rightarrow e\tau$ have somewhat smaller BRs $\lesssim \mathcal{O}(10^{-11})$, but still within experimental sensitivity. (Notice that points with associated $\text{BR}(Z \rightarrow \ell_1^\mp \ell_2^\pm)$ within FCC-ee reach are cosmologically disfavoured in contrast to what was encountered in the study of the simple toy model of Section 4.) Again, even though we only display the NH for the light neutrino spectrum, our numerical results show that the corresponding prospects for $\text{BR}(Z \rightarrow \ell_1^\mp \ell_2^\pm)$ would be similar in an IH case.

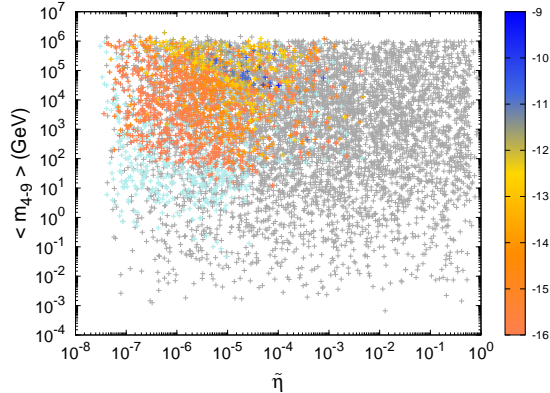


Figure 9: ISS realisation: maximal values of $\text{BR}(Z \rightarrow \ell_1^\mp \ell_2^\pm)$ on the $(\tilde{\eta}, \langle m_{4-9} \rangle)$ parameter space for a NH light neutrino spectrum, from larger (dark blue) to smaller (orange) values. Cyan denotes values of the branching fractions below 10^{-18} .

Just as previously done, we summarise the prospects for the observation of cLFV Z decays in the framework of the ISS by considering the $(\tilde{\eta}, \langle m_{4-9} \rangle)$ parameter space of this specific realisation; this is illustrated in Fig. 9, for a NH light neutrino spectrum.

The complementarity of low-energy LFV observables and LFV Z decays at a high-luminosity Z factory for this ISS realisation is displayed in Fig. 10, where we further highlight points that can potentially account for a $0\nu 2\beta$ rate within sensitivity of future experiments. The results are in agreement with the findings for the “3+1 model”: low-energy experiments - as COMET looking for $\mu - e$ conversion in Al nuclei - are better probes of cLFV in the $\mu - e$ sector of this (3,3) ISS realisation; on the other hand, a future high-luminosity Z factory has a stronger power to probe LFV in the $\mu - \tau$ sector via Z decays.

7 Overview

In this work we have explored indirect searches for sterile neutrinos at a future circular collider running in the electron positron mode. In particular, we have considered the impact of sterile neutrinos for (very) rare cLFV Z decays, which can be probed by the FCC-ee (TLEP) running close to the Z mass threshold, with an expected sensitivity to $\text{BR}(Z \rightarrow \ell_1^\mp \ell_2^\pm)$ as low as 10^{-13} .

While these rare decays are forbidden in the SM (and have tiny BRs in its ad-hoc extensions where neutrino masses and mixings are put by hand), in models where the SM is extended via additional neutral sterile fermions, which have non-negligible mixings with the active (light) states, one can have significant contributions to cLFV Z decays.

We have considered here three scenarios with sterile neutrinos: a minimal “3+1 toy model”, and two frameworks for neutrino mass generation, the ν MSM and the ISS. In our analysis we have conducted a thorough (numerical) exploration of the parameter space of the different models: we take into account recent data on neutrino oscillations, as well as numerous experimental and observational constraints on the sterile states. As hinted by early analytical studies, and as a consequence of the common LFV $Z\ell_1^\mp \ell_2^\pm$ vertex, low-energy cLFV observables receiving contributions from Z -mediated penguins impose strong constraints on the sterile neutrino induced $\text{BR}(Z \rightarrow \ell_1^\mp \ell_2^\pm)$.

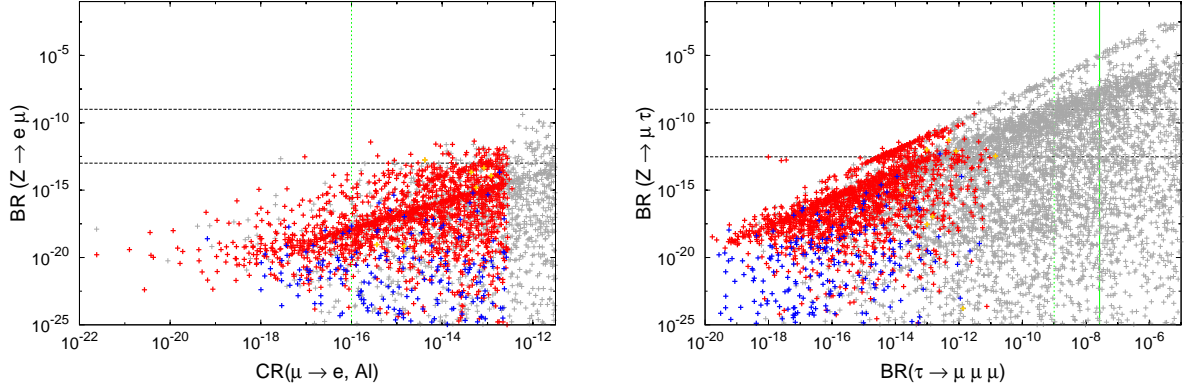


Figure 10: ISS realisation: on the left, $\text{BR}(Z \rightarrow e\mu)$ versus $\text{CR}(\mu - e, \text{Al})$ and on the right $\text{BR}(Z \rightarrow \mu\tau)$ versus $\text{BR}(\tau 3\mu)$, for a NH light neutrino spectrum. Line and colour code as in Fig. 2. When present, the additional green vertical lines denote the current bounds (solid) and future sensitivity (dashed), and dark-yellow points denote an associated $|m_{ee}|$ within experimental reach.

The very minimal sterile extension of the SM - the “3+1 model” - clearly illustrates the potential of the FCC-ee to probe the sterile neutrino contributions to LFV Z decays: both $\text{BR}(Z \rightarrow \mu\tau)$ and $\text{BR}(Z \rightarrow e\tau)$ are well within reach, especially for sterile masses $\gtrsim 100$ GeV, and for sterile mixing angles $\theta_{i4} > 10^{-6}$. Our analysis further emphasised the underlying synergy between a high-luminosity Z factory and other dedicated (low-energy) facilities: regions in “3+1 model” parameter space can be probed via cLFV Z decays at FCC-ee, through cLFV low-energy decays ($\tau \rightarrow 3\mu$) and neutrinoless double beta decays within reach of future dedicated facilities (the latter especially in the case of an IH light neutrino spectrum); moreover, a high-luminosity Z factory could probe LFV in the $\mu - \tau$ sector, clearly going beyond the reach of low-energy facilities. Similar prospects were found for a (3,3) Inverse Seesaw realisation. In contrast, the νMSM parameter space favoured by a successful generation of the observed BAU turns out to be associated to very small values of $\text{BR}(Z \rightarrow \ell_1^\mp \ell_2^\pm)$, beyond the reach of the FCC-ee. Nevertheless, direct searches for νMSM sterile states can be carried at FCC-ee (for instance displaced vertices associated to long-lived RH neutrinos [37]). We have also considered the violation of lepton flavour universality in Z decays, as encoded by the quantity ΔR_Z^{lep} . Still, in all the models here considered, the estimated contributions of the sterile fermions to this observable lie beyond experimental reach.

Our analysis reveals that sterile neutrinos can indeed give rise to contributions to $\text{BR}(Z \rightarrow \ell_1^\mp \ell_2^\pm)$ within reach of the FCC-ee; these studies, in parallel with other direct searches, have the potential to integrate the physics case of FCC-ee (TLEP). Nevertheless, the results summarised here consisted only of a first theoretical study: a full discussion and estimation of the different backgrounds, accompanied by simulations of the events and the detector(s) will be required to ascertain whether or not one can indeed have LFV signals above the background. This will be done in a subsequent work.

Acknowledgements

We are very grateful to Y. Kuno for his helpful comments and suggestions. We also thank S. Davidson for enlightening discussions. The authors acknowledge support from the European Union FP7 ITN INVISIBLES (Marie Curie Actions, PITN-GA-2011-289442). This work was done in the framework of a “PEPS PTI 2014” project.

A Loop integrals

The two- and three-point one-loop dimensionless functions are defined as:

$$\mathbb{B}_1(x_i) \equiv B_1(0; m_i^2, M_W^2), \quad (42)$$

$$\bar{\mathbb{C}}_..(x_i) \equiv M_W^2 C_..(0, Q^2, 0; m_i^2, M_W^2, M_W^2), \quad (43)$$

$$\mathbb{C}_..(x_i, x_j) \equiv M_W^2 C_..(0, Q^2, 0; M_W^2, m_i^2, m_j^2), \quad (44)$$

from the usual loop integrals [45, 46] with the tensor decomposition (Minkowski metric):

$$B^\mu(p^2; m_0^2, m_1^2) = p^\mu B_1, \quad (45)$$

$$C^\mu(p_1^2, Q^2, p_2^2; m_0^2, m_1^2, m_2^2) = p_1^\mu C_{11} + p_2^\mu C_{12}, \quad (46)$$

$$C^{\mu\nu}(p_1^2, Q^2, p_2^2; m_0^2, m_1^2, m_2^2) = p_1^\mu p_1^\nu C_{21} + p_2^\mu p_2^\nu C_{22} + (p_1^\mu p_2^\nu + p_2^\mu p_1^\nu) C_{23} + g^{\mu\nu} M_W^2 C_{24}. \quad (47)$$

References

- [1] S. L. Glashow, J. Iliopoulos, and L. Maiani, *Phys. Rev. D* **2** (1970) 1285.
- [2] T. Riemann and G. Mann, “Nondiagonal Z decay: $Z \rightarrow e\mu$ ”, in *Proc. of the Int. Conf. Neutrino’82, 14-19 June 1982, Balatonfüred, Hungary* (A. Frenkel and E. Jenik, eds.), vol. II, pp. 58–61, Budapest, 1982, scanned copy at <http://www.ifh.de/~riemann>.
- [3] G. Mann and T. Riemann, *Ann. Phys.* **40** (1984) 334.
- [4] T. Riemann, “FCNC and $Z \rightarrow e\mu, \mu\tau, \tau e$ and the LC at the Z peak”, talk at *DESY-ECFA LC Workshop* held at Oxford, March 20-23
- [5] J. I. Illana, M. Jack and T. Riemann, “Predictions for $Z \rightarrow \mu\tau$ and related reactions,” in *2nd ECFA/DESY Study 1998-2001*, 490-524 [hep-ph/0001273].
- [6] M. A. Acero, C. Giunti and M. Laveder, *Phys. Rev. D* **78** (2008) 073009 [arXiv:0711.4222 [hep-ph]]; C. Giunti and M. Laveder, *Phys. Rev. C* **83** (2011) 065504 [arXiv:1006.3244 [hep-ph]].
- [7] T. A. Mueller, D. Lhuillier, M. Fallot, A. Letourneau, S. Cormon, M. Fechner, L. Giot and T. Lasserre *et al.*, *Phys. Rev. C* **83** (2011) 054615 [arXiv:1101.2663 [hep-ex]]; P. Huber, *Phys. Rev. C* **84** (2011) 024617 [Erratum-ibid. *C* **85** (2012) 029901] [arXiv:1106.0687 [hep-ph]]; G. Mention, M. Fechner, T. Lasserre, T. A. Mueller, D. Lhuillier, M. Cribier and A. Letourneau, *Phys. Rev. D* **83** (2011) 073006 [arXiv:1101.2755 [hep-ex]].
- [8] A. A. Aguilar-Arevalo *et al.* [LSND Collaboration], *Phys. Rev. D* **64** (2001) 112007 [hep-ex/0104049].

- [9] A. A. Aguilar-Arevalo *et al.* [MiniBooNE Collaboration], Phys. Rev. Lett. **98** (2007) 231801 [arXiv:0704.1500 [hep-ex]]; A. A. Aguilar-Arevalo *et al.* [MiniBooNE Collaboration], Phys. Rev. Lett. **105** (2010) 181801 [arXiv:1007.1150 [hep-ex]]; A. A. Aguilar-Arevalo *et al.* [MiniBooNE Collaboration], Phys. Rev. Lett. **110** (2013) 161801 [arXiv:1207.4809 [hep-ex], arXiv:1303.2588 [hep-ex]].
- [10] S. Dodelson and L. M. Widrow, Phys. Rev. Lett. **72** (1994) 17 [hep-ph/9303287].
- [11] K. Abazajian, G. M. Fuller and M. Patel, Phys. Rev. D **64** (2001) 023501 [astro-ph/0101524].
- [12] A. D. Dolgov and S. H. Hansen, Astropart. Phys. **16** (2002) 339 [hep-ph/0009083]; A. Boyarsky, J. Lesgourgues, O. Ruchayskiy and M. Viel, Phys. Rev. Lett. **102** (2009) 201304 [arXiv:0812.3256 [hep-ph]]; A. Boyarsky, O. Ruchayskiy and M. Shaposhnikov, Ann. Rev. Nucl. Part. Sci. **59** (2009) 191 [arXiv:0901.0011 [hep-ph]].
- [13] A. A. Klypin, A. V. Kravtsov, O. Valenzuela and F. Prada, Astrophys. J. **522** (1999) 82 [astro-ph/9901240]; B. Moore, S. Ghigna, F. Governato, G. Lake, T. R. Quinn, J. Stadel and P. Tozzi, Astrophys. J. **524** (1999) L19 [astro-ph/9907411]; L. E. Strigari, C. S. Frenk and S. D. M. White, Mon. Not. Roy. Astron. Soc. **408** (2010) 2364 [arXiv:1003.4268 [astro-ph.CO]]; M. Boylan-Kolchin, J. S. Bullock and M. Kaplinghat, Mon. Not. Roy. Astron. Soc. **415** (2011) L40 [arXiv:1103.0007 [astro-ph.CO]].
- [14] P. A. R. Ade *et al.* [Planck Collaboration], Astron. Astrophys. **571** (2014) A16 [arXiv:1303.5076 [astro-ph.CO]].
- [15] G. Mann and T. Riemann, Annalen Phys. **40** (1984) 334.
- [16] J. I. Illana and T. Riemann, Phys. Rev. D **63** (2001) 053004 [hep-ph/0010193].
- [17] A. Ilakovac and A. Pilaftsis, Nucl. Phys. B **437** (1995) 491 [hep-ph/9403398].
- [18] M. A. Perez, G. Tavares-Velasco and J. J. Toscano, Int. J. Mod. Phys. A **19** (2004) 159 [hep-ph/0305227].
- [19] A. Flores-Tlalpa, J. M. Hernandez, G. Tavares-Velasco and J. J. Toscano, Phys. Rev. D **65** (2002) 073010 [hep-ph/0112065].
- [20] D. Delepine and F. Vissani, Phys. Lett. B **522** (2001) 95 [hep-ph/0106287].
- [21] S. Davidson, S. Lacroix and P. Verdier, JHEP **1209** (2012) 092 [arXiv:1207.4894 [hep-ph]].
- [22] G. Aad *et al.* [ATLAS Collaboration], Phys. Rev. D **90** (2014) 7, 072010 [arXiv:1408.5774 [hep-ex]].
- [23] O. Adriani *et al.* [L3 Collaboration], Phys. Lett. B **316** (1993) 427.
- [24] R. Akers *et al.* [OPAL Collaboration], Z. Phys. C **67** (1995) 555.
- [25] P. Abreu *et al.* [DELPHI Collaboration], Z. Phys. C **73** (1997) 243.
- [26] Work done in the framework of the Flavour Physics Working Group of the FCC-ee design study, <http://tlep.web.cern.ch/>

- [27] D. V. Forero, M. Tortola and J. W. F. Valle, Phys. Rev. D **86** (2012) 073012 [arXiv:1205.4018 [hep-ph]].
- [28] G. L. Fogli, E. Lisi, A. Marrone, D. Montanino, A. Palazzo and A. M. Rotunno, Phys. Rev. D **86** (2012) 013012 [arXiv:1205.5254 [hep-ph]].
- [29] M. C. Gonzalez-Garcia, M. Maltoni, J. Salvado and T. Schwetz, JHEP **1212** (2012) 123 [arXiv:1209.3023 [hep-ph]].
- [30] D. V. Forero, M. Tortola and J. W. F. Valle, Phys. Rev. D **90** (2014) 093006 [arXiv:1405.7540 [hep-ph]].
- [31] See also <http://www.nu-fit.org/>
- [32] M. C. Gonzalez-Garcia, M. Maltoni and T. Schwetz, JHEP **1411** (2014) 052 [arXiv:1409.5439 [hep-ph]].
- [33] J. Adam *et al.* [MEG Collaboration], Phys. Rev. Lett. **110** (2013) 201801 [arXiv:1303.0754 [hep-ex]].
- [34] A. Abada, D. Das, A. M. Teixeira, A. Vicente and C. Weiland, JHEP **1302** (2013) 048 [arXiv:1211.3052 [hep-ph]].
- [35] A. Abada, A. M. Teixeira, A. Vicente and C. Weiland, JHEP **1402** (2014) 091 [arXiv:1311.2830 [hep-ph]].
- [36] A. Abada, V. De Romeri and A. M. Teixeira, JHEP **1409** (2014) 074 [arXiv:1406.6978 [hep-ph]].
- [37] A. Blondel *et al.* [team for the FCC-ee study Collaboration], “Search for Heavy Right Handed Neutrinos at the FCC-ee,” arXiv:1411.5230 [hep-ex].
- [38] T. Asaka, S. Blanchet and M. Shaposhnikov, Phys. Lett. B **631** (2005) 151 [hep-ph/0503065].
- [39] R. N. Mohapatra and J. W. F. Valle, Phys. Rev. D **34** (1986) 1642.
- [40] E. Fernandez-Martinez, M. B. Gavela, J. Lopez-Pavon and O. Yasuda, Phys. Lett. B **649** (2007) 427 [hep-ph/0703098].
- [41] J. Schechter and J. W. F. Valle, Phys. Rev. D **22** (1980) 2227.
- [42] M. Gronau, C. N. Leung and J. L. Rosner, Phys. Rev. D **29** (1984) 2539.
- [43] T. Hahn and M. Perez-Victoria, Comput. Phys. Commun. **118** (1999) 153 [hep-ph/9807565].
- [44] G. J. van Oldenborgh, Comput. Phys. Commun. **66** (1991) 1.
- [45] G. 't Hooft and M. Veltman, Nucl. Phys. B **44** (1972) 189–213.
- [46] G. Passarino and M. Veltman, Nucl. Phys. B **160** (1979) 151.
- [47] A. Freitas, JHEP **1404** (2014) 070 [arXiv:1401.2447 [hep-ph]].
- [48] K. A. Olive *et al.* [Particle Data Group Collaboration], Chin. Phys. C **38** (2014) 090001 [arXiv:1412.1408 [astro-ph.CO]].

- [49] M. Bicer *et al.*, JHEP **1401** (2014) 164 [arXiv:1308.6176 [hep-ex]].
- [50] G. Wilson, “Neutrino oscillations: are lepton-flavor violating Z decays observable with the CDR detector?” and “Update on experimental aspects of lepton-flavour violation”, talks at DESY-ECFA LC Workshops held at Frascati, November 1998 and at Oxford, March 1999.
- [51] S. Schael *et al.*, Phys. Rept. **427** (2006) 257-454 [hep-ex/0509008].
- [52] A. Ibarra, E. Molinaro and S. T. Petcov, JHEP **1009** (2010) 108 [arXiv:1007.2378 [hep-ph]].
- [53] F. Capozzi, G. L. Fogli, E. Lisi, A. Marrone, D. Montanino and A. Palazzo, Phys. Rev. D **89** (2014) 093018 [arXiv:1312.2878 [hep-ph]].
- [54] S. Antusch, J. P. Baumann and E. Fernandez-Martinez, Nucl. Phys. B **810** (2009) 369 [arXiv:0807.1003 [hep-ph]].
- [55] S. Antusch and O. Fischer, JHEP **1410** (2014) 94 [arXiv:1407.6607 [hep-ph]].
- [56] F. del Aguila, J. de Blas and M. Perez-Victoria, Phys. Rev. D **78** (2008) 013010 [arXiv:0803.4008 [hep-ph]].
- [57] E. Akhmedov, A. Kartavtsev, M. Lindner, L. Michaels and J. Smirnov, JHEP **1305** (2013) 081 [arXiv:1302.1872 [hep-ph]].
- [58] L. Basso, O. Fischer and J. J. van der Bij, Europhys. Lett. **105** (2014) 11001 [arXiv:1310.2057 [hep-ph]].
- [59] P. S. Bhupal Dev, R. Franceschini and R. N. Mohapatra, Phys. Rev. D **86** (2012) 093010 [arXiv:1207.2756 [hep-ph]].
- [60] C. G. Cely, A. Ibarra, E. Molinaro and S. T. Petcov, Phys. Lett. B **718** (2013) 957 [arXiv:1208.3654 [hep-ph]].
- [61] P. Bandyopadhyay, E. J. Chun, H. Okada and J. -C. Park, JHEP **1301** (2013) 079 [arXiv:1209.4803 [hep-ph]].
- [62] E. Goudzovski [NA48/2 and NA62 Collaborations], PoS EPS **-HEP2011** (2011) 181 [arXiv:1111.2818 [hep-ex]].
- [63] C. Lazzeroni *et al.* [NA62 Collaboration], Phys. Lett. B **719** (2013) 326 [arXiv:1212.4012 [hep-ex]].
- [64] P. Naik *et al.* [CLEO Collaboration], Phys. Rev. D **80** (2009) 112004 [arXiv:0910.3602 [hep-ex]].
- [65] H. -B. Li, “Proceedings, 4th International Workshop on Charm Physics (Charm 2010) : Beijing, China, October 21-24, 2010,” Int. J. Mod. Phys. Conf. Ser. **02** (2011).
- [66] B. Aubert *et al.* [BaBar Collaboration], Phys. Rev. D **77** (2008) 011107.
- [67] I. Adachi *et al.* [Belle Collaboration], Phys. Rev. Lett. **110** (2013) 131801 [arXiv:1208.4678 [hep-ex]].
- [68] A. Kusenko, Phys. Rept. **481** (2009) 1 [arXiv:0906.2968 [hep-ph]].

- [69] A. Atre, T. Han, S. Pascoli and B. Zhang, JHEP **0905** (2009) 030 [arXiv:0901.3589 [hep-ph]].
- [70] E. Ma and A. Pramudita, Phys. Rev. D **22** (1980) 214.
- [71] F. Deppisch and J. W. F. Valle, Phys. Rev. D **72** (2005) 036001 [hep-ph/0406040].
- [72] F. Deppisch, T. S. Kosmas and J. W. F. Valle, Nucl. Phys. B **752** (2006) 80 [hep-ph/0512360].
- [73] D. N. Dinh, A. Ibarra, E. Molinaro and S. T. Petcov, Decays and TeV Scale See-Saw Scenarios of Neutrino Mass Generation,” JHEP **1208** (2012) 125 [Erratum-ibid. **1309** (2013) 023] [arXiv:1205.4671 [hep-ph]].
- [74] R. Alonso, M. Dhen, M. B. Gavela and T. Hambye, JHEP **1301** (2013) 118 [arXiv:1209.2679 [hep-ph]].
- [75] A. Abada, M. E. Krauss, W. Porod, F. Staub, A. Vicente and C. Weiland, JHEP **1411** (2014) 048 [arXiv:1408.0138 [hep-ph]].
- [76] A. M. Baldini, F. Cei, C. Cerri, S. Dussoni, L. Galli, M. Grassi, D. Nicolo and F. Raffaelli *et al.*, arXiv:1301.7225 [physics.ins-det].
- [77] B. Aubert *et al.* [BaBar Collaboration], Phys. Rev. Lett. **104** (2010) 021802
- [78] T. Aushev, W. Bartel, A. Bondar, J. Brodzicka, T. E. Browder, P. Chang, Y. Chao and K. F. Chen *et al.*, “Physics at Super B Factory,” arXiv:1002.5012 [hep-ex].
- [79] U. Bellgardt *et al.* [SINDRUM Collaboration], Nucl. Phys. B **299** (1988) 1.
- [80] A. Blondel, A. Bravar, M. Pohl, S. Bachmann, N. Berger, M. Kiehn, A. Schoning and D. Wiedner *et al.*, “Research Proposal for an Experiment to Search for the Decay $\mu \rightarrow eee$,” arXiv:1301.6113 [physics.ins-det].
- [81] K. Hayasaka, K. Inami, Y. Miyazaki, K. Arinstein, V. Aulchenko, T. Aushev, A. M. Bakich and A. Bay *et al.*, Phys. Lett. B **687** (2010) 139 [arXiv:1001.3221 [hep-ex]].
- [82] C. Dohmen *et al.* [SINDRUM II. Collaboration], Phys. Lett. B **317** (1993) 631.
- [83] A. Alekou, R. Appleby, M. Aslaninejad, R. J. Barlow, R. C. K. M. Hock, J. Garland, L. J. Jenner and D. J. Kelliher *et al.*, “Accelerator system for the PRISM based muon to electron conversion experiment,” arXiv:1310.0804 [physics.acc-ph].
- [84] W. H. Bertl *et al.* [SINDRUM II Collaboration], Eur. Phys. J. C **47** (2006) 337.
- [85] Y. Kuno [COMET Collaboration], PTEP **2013** (2013) 022C01.
- [86] P. Benes, A. Faessler, F. Simkovic and S. Kovalenko, Phys. Rev. D **71** (2005) 077901 [hep-ph/0501295].
- [87] M. Blennow, E. Fernandez-Martinez, J. Lopez-Pavon and J. Menendez, JHEP **1007** (2010) 096 [arXiv:1005.3240 [hep-ph]].
- [88] M. Agostini *et al.* [GERDA Collaboration], Phys. Rev. Lett. **111** (2013) 12, 122503 [arXiv:1307.4720 [nucl-ex]].

- [89] M. Auger *et al.* [EXO Collaboration], Phys. Rev. Lett. **109** (2012) 032505 [arXiv:1205.5608 [hep-ex]].
- [90] J. B. Albert *et al.* [EXO-200 Collaboration], Nature **510** (2014) 229-234 [arXiv:1402.6956 [nucl-ex]].
- [91] A. Gando *et al.* [KamLAND-Zen Collaboration], Phys. Rev. Lett. **110** (2013) 062502 [arXiv:1211.3863 [hep-ex]].
- [92] [Delia Tosi on behalf of the EXO Collaboration], “The search for neutrino-less double-beta decay: summary of current experiments,” arXiv:1402.1170 [nucl-ex].
- [93] P. Gorla [CUORE Collaboration], J. Phys. Conf. Ser. **375** (2012) 042013.
- [94] D. R. Artusa *et al.* [CUORE Collaboration], “Searching for neutrinoless double-beta decay of ^{130}Te with CUORE,” arXiv:1402.6072 [physics.ins-det].
- [95] J. Hartnell [SNO+ Collaboration], J. Phys. Conf. Ser. **375** (2012) 042015 [arXiv:1201.6169 [physics.ins-det]].
- [96] A. Barabash [SuperNEMO Collaboration], J. Phys. Conf. Ser. **375** (2012) 042012.
- [97] F. Granena *et al.* [NEXT Collaboration], “NEXT, a HPGXe TPC for neutrinoless double beta decay searches,” arXiv:0907.4054 [hep-ex].
- [98] J. J. Gomez-Cadenas *et al.* [NEXT Collaboration], “Present status and future perspectives of the NEXT experiment,” arXiv:1307.3914 [physics.ins-det].
- [99] J. F. Wilkerson, E. Aguayo, F. T. Avignone, H. O. Back, A. S. Barabash, J. R. Beene, M. Bergevin and F. E. Bertrand *et al.*, J. Phys. Conf. Ser. **375** (2012) 042010.
- [100] A. Y. Smirnov and R. Zukanovich Funchal, Phys. Rev. D **74** (2006) 013001 [hep-ph/0603009].
- [101] E. Bulbul, M. Markevitch, A. Foster, R. K. Smith, M. Loewenstein and S. W. Randall, Astrophys. J. **789** (2014) 13 [arXiv:1402.2301 [astro-ph.CO]].
- [102] A. Boyarsky, O. Ruchayskiy, D. Iakubovskiy and J. Franse, Phys. Rev. Lett. [arXiv:1402.4119 [astro-ph.CO]].
- [103] K. N. Abazajian, M. A. Acero, S. K. Agarwalla, A. A. Aguilar-Arevalo, C. H. Albright, S. Antusch, C. A. Argüelles and A. B. Balantekin *et al.*, “Light Sterile Neutrinos: A White Paper,” arXiv:1204.5379 [hep-ph].
- [104] B. Dasgupta and J. Kopp, Phys. Rev. Lett. **112** (2014) 031803 [arXiv:1310.6337 [hep-ph]].
- [105] G. Gelmini, E. Osoba, S. Palomares-Ruiz and S. Pascoli, JCAP **0810** (2008) 029 [arXiv:0803.2735 [astro-ph]].
- [106] M. S. Chanowitz, M. A. Furman and I. Hinchliffe, Nucl. Phys. B **153** (1979) 402.
- [107] L. Durand, J. M. Johnson and J. L. Lopez, Phys. Rev. Lett. **64** (1990) 1215.
- [108] J. G. Korner, A. Pilaftsis and K. Schilcher, Phys. Lett. B **300** (1993) 381 [hep-ph/9301290].

- [109] J. Bernabeu, J. G. Korner, A. Pilaftsis and K. Schilcher, Phys. Rev. Lett. **71** (1993) 2695 [hep-ph/9307295].
- [110] S. Fajfer and A. Ilakovac, Phys. Rev. D **57** (1998) 4219.
- [111] A. Ilakovac, Phys. Rev. D **62** (2000) 036010 [hep-ph/9910213].
- [112] T. Asaka and M. Shaposhnikov, Phys. Lett. B **620** (2005) 17 [hep-ph/0505013].
- [113] M. Shaposhnikov, JHEP **0808** (2008) 008 [arXiv:0804.4542 [hep-ph]].
- [114] L. Canetti, M. Drewes, T. Frossard and M. Shaposhnikov, Phys. Rev. D **87** (2013) 9, 093006 [arXiv:1208.4607 [hep-ph]].
- [115] E. K. Akhmedov, V. A. Rubakov and A. Y. Smirnov, Phys. Rev. Lett. **81** (1998) 1359 [hep-ph/9803255].
- [116] M. Laine and M. Shaposhnikov, JCAP **0806** (2008) 031 [arXiv:0804.4543 [hep-ph]].
- [117] A. Pilaftsis and T. E. J. Underwood, Nucl. Phys. B **692** (2004) 303 [hep-ph/0309342].
- [118] G. Bernardi, G. Carugno, J. Chauveau, F. Dicarolo, M. Dris, J. Dumarchez, M. Ferro-Luzzi and J. M. Levy *et al.*, Phys. Lett. B **166** (1986) 479.
- [119] G. Bernardi, G. Carugno, J. Chauveau, F. Dicarolo, M. Dris, J. Dumarchez, M. Ferro-Luzzi and J.-M. Levy *et al.*, Phys. Lett. B **203** (1988) 332.
- [120] L. Canetti and M. Shaposhnikov, Hyperfine Interact. **214** (2013) 1-3, 5.
- [121] W. Bonivento, A. Boyarsky, H. Dijkstra, U. Egede, M. Ferro-Luzzi, B. Goddard, A. Golutvin and D. Gorbunov *et al.*, arXiv:1310.1762 [hep-ex].
- [122] A. Abada and M. Lucente, Nucl. Phys. B **885** (2014) 651 [arXiv:1401.1507 [hep-ph]].
- [123] A. Abada, G. Arcadi and M. Lucente, JCAP **1410** (2014) 001 [arXiv:1406.6556 [hep-ph]].
- [124] M. C. Gonzalez-Garcia and J. W. F. Valle, Phys. Lett. B **216** (1989) 360.
- [125] J. A. Casas and A. Ibarra, Nucl. Phys. B **618** (2001) 171 [hep-ph/0103065].
- [126] D. V. Forero, S. Morisi, M. Tortola and J. W. F. Valle, JHEP **1109** (2011) 142 [arXiv:1107.6009 [hep-ph]].
- [127] M. Malinsky, T. Ohlsson and H. Zhang, Phys. Rev. D **79** (2009) 073009 [arXiv:0903.1961 [hep-ph]].
- [128] P. S. B. Dev and R. N. Mohapatra, Phys. Rev. D **81** (2010) 013001 [arXiv:0910.3924 [hep-ph]].